United Arab Emirates University

Scholarworks@UAEU

4-2021

CONTROLLABILITY AND OBSERVABILITY OF BLOOD GLUCOSE LEVELS AND THE IMPACT OF COVID-19 ON DIABETIC PATIENTS

Mahra Salem Nasser Abdulla Alblooshi

United Arab Emirates University

College of Science

Department of Mathematical Sciences

CONTROLLABILITY AND OBSERVABILITY OF BLOOD GLUCOSE LEVELS AND THE IMPACT OF COVID-19 ON DIABETIC PATIENTS

Mahra Salem Nasser Abdulla Alblooshi

This thesis is submitted in partial fulfillment of the requirements for the degree of Master of Science in Mathematics
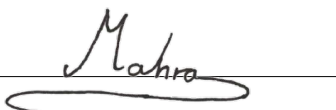
Under the Supervision of Dr. Abdessamad Tridane

April 2021

Declaration of Original Work

I, Mahra Salem Nasser Abdulla Alblooshi, the undersigned, a graduate student at the United Arab Emirates University (UAEU), and the author of this thesis, entitled *"Controllability and Observability of Blood Glucose Levels and the Impact of COVID-19 on Diabetic Patients"*, hereby, solemnly declare that this thesis is my own original research work that has been done and prepared by me under the supervision of Dr. Abdessamad Tridane, in the College of Science at UAEU. This work has not previously formed the basis for the award of any academic degree, diploma or a similar title at this or any other university. Any materials borrowed from other sources (whether published or unpublished) and relied upon or included in my thesis have been properly cited and acknowledged in accordance with appropriate academic conventions. I further declare that there is no potential conflict of interest with respect to the research, data collection, authorship, presentation and/or publication of this thesis.

Student's Signature _____   Date ___August 27, 2021___

Approval of the Master Thesis

This Master Thesis is approved by the following Examining Committee Members:

1) Advisor (Committee Chair): Abdessamad Tridane

   Title: Associate Professor

   Department of Mathematical Sciences

   College of Science

   Signature _____ Date __April 25,2021__
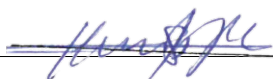
2) Member: Mohamed Ali Hajji

   Title: Associate Professor

   Department of Mathematical Sciences

   College of Science
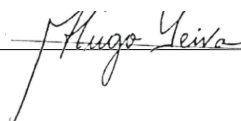
   Signature _____ Date __June 21, 2021__

3) Member (External Examiner): Hugo Leiva

   Title: Full Professor

   Yachay Tech-University, Ecuador

   Signature _____ Date __June 21, 2021__

This Master Thesis is accepted by:

Dean of the College of Science: Professor Maamar Benkraouda

Signature _maamar Benkraouda_   Date August 31, 2021

Dean of the College of Graduate Studies: Professor Ali Al-Marzouqi

Signature ___Ali Hassan___   Date _August 31, 2021_

Copy ____ of ____

Abstract

Diabetes is a metabolic disorder that is characterized by high blood glucose concentrations resulting from insulin deficiency in case of type 1 or insulin inefficiency in case of type 2. While no cure for diabetes exists, the artificial pancreas is a possible way to manage diabetes, especially for type 1 diabetics. Where an artificial pancreas is a closed loop control system with an integrated mathematical model. This control system imitates the function of a healthy pancreas. The first part of this thesis is concerned with the control system of an artificial pancreas that is based on Bergman's minimal model of the glucose-insulin dynamics. The aim of the first part of this thesis is to prove both the controllability and the observability of the minimal model which is an fundamental step in the design of an optimal control system. These proofs are based on several mathematical tools such as the insertion of time delays, and theorems such as the Banach contraction mapping theorem in addition to the results of previous related works.

On a different note, COVID-19 is a highly infectious global pandemic that targets the respiratory system. The symptoms of this disease were found to be more severe towards patients with comorbidities including diabetes, and so, the second part of this thesis is concerned with the relation of COVID-19 with comorbidities, where a COVID-19 disease transmission model that focuses on comorbidity populations is presented. This model aims at determining the major factors that contributes to the transmission of this disease. The results of this model can aid in implementing strategies that can help in controlling the spread of this pandemic. Parameter estimations of the model are presented in addtion to several related calculations including the basic reproduction number and the sensitivity indices of the model's parameters.

Keywords: Diabetes, Control systems, Controllability, Observability, COVID-19, Compartmental disease transmission models, Sensitivity index, Basic reproduction number.

Title and Abstract (in Arabic)

القدرة على التحكم بمستوى الجلوكوز بالدم و قابلية مراقبته و تأثير كوفيد-19 على مرضى السكري

الملخص

مرض السكري هو اضطراب في عملية الأيض يتصف بارتفاع مستوى الجلوكوز بالدم الناتج عن نقص مستوى الإنسولين في حالة النوع الأول أو عدم كفاءة الإنسولين في النوع الثاني. في حين لايوجد علاج لمرضى السكري، يعتبر البنكرياس الصناعي طريقة ممكنة لإدارة المرض و خصوصاً لمرضى السكري من النوع الأول. و يُعرّف البنكرياس الصناعي على أنه نظام تحكم مغلق قائم على نموذج رياضي معين. يعمل هذا النظام على محاكاة وظيفة البنكرياس السليم. الجزء الأول من هذه الأطروحة يهتم بنظام التحكم الخاص بالبنكرياس الصناعي الذي يستخدم نموذج برجمان البسيط كنموذج رياضي خاص بديناميات الجلوكوز و الإنسولين. الهدف من الجزء الأول من هذه الأطروحة هو إثبات كلاً من إمكانية التحكم و إمكانية المراقبة المتعلقة بنموذج برجمان البسيط و هي خطوة أساسية في تصميم نظام تحكم أمثل. البراهين المقدمة في هذه الأطروحة مبنية على عدة أدوات رياضية مثل إدراج التأخيرات الزمنية في النموذج و نظريات مثل نظرية النقطة الثابتة لباناخ بالإضافة إلى نتائج الأعمال السابقة ذات الصلة.

من ناحية أخرى، يُعرف كوفيد-19 بأنه جائحة عالمية شديدة العدوى تستهدف النظام التنفسي. وُجد أن أعراض هذا المرض تبدو أكثر حدة تجاه المرضى الذين يعانون من أمراض مصاحبة بما في ذلك مرض السكري. ولذلك يهتم الجزء الثاني من هذه الأطروحة بعلاقة مرض كوفيد-19 بالأمراض المصاحبة حيث تم تقديم نموذج انتقال المرض الخاص بكوفيد-19 الذي يركز على السكان المصابين بالأمراض المصاحبة. يهدف هذا النموذج إلى تحديد العوامل الرئيسية التي تساهم في انتشار هذا المرض. النتائج التي يقدمها هذا النموذج قد تساعد في انشاء الاستراتيجيات التي تساهم في السيطرة على انتشار هذا المرض. هذا الجزء من الأطروحة يحتوي على تقدير قيم المعاملات الخاصة بالنموذج بالإضافة إلى حسابات ذات صلة مثل عدد التكاثر الأساسي و موشر حساسية المعاملات الخاصة بالنموذج.

مفاهيم البحث الرئيسية: مرض السكري، أنظمة التحكم، القدرة على التحكم، قابلية الملاحظة، كوفيد-19، نماذج انتقال المرض المجزأة، مؤشر الحساسية، عدد التكاثر الأساسي.

Acknowledgements

First of all, I would not have been able to finish this thesis without the help of God as he granted me the patience, knowledge, ability and opportunity to do so.

Next, I would like to thank my supervisor Dr. Abdessamad for his guidance throughout my work on this thesis. I am especially grateful for Prof. Hugo Leiva from Yachay Tech University who has enormous knowledge in the control theory field with many related publications, for his substantial contribution in proving the controllability and the observability of the bergman model presented in the first part of this thesis. My thanks also extends to Dr. Salih Djilali from Hassiba Benbouali University for his contributions in fitting the COVID-19 model presented in the second part of this thesis, in addition to his contributions in other MATLAB related work.

Further, I would like to thank Dr. Adama Diene, chairman of the Department of Mathematical Sciences at the United Arab Emirates University, for his continuous encouragement, and I would also like to thank Dr. Ahmed Al-Rawashdeh, coordinator of the master program of the department for his support, encouragement, assistance and guidance as well as his equity and ability to impart knowledge as a faculty instructor.

My thanks also extends to my professors, Prof. Muhammed Syam, Dr. Mohamed Ali Hajji and Prof. Qasem Al-Mdallal for their encouragement, support and for educating me on many different applied mathematical concepts.

Last but not least, I would like to thank my family, cousins and friends for their continuous moral support, especially my mother whom I am really grateful for.

Dedication

To my precious parents and dear siblings

Table of Contents

List of Tables

List of Figures

List of Abbreviations

CGM	Continuous Glucose Monitor
COVID-19	Corona Virus Disease 2019
ICU	Intensive Care Unit
IDF	International Diabetes Federation
IVGTT	Intravenous Glucose Tolerance Test
MENA	Middle East and North Africa
MERS	Middle East Respiratory Syndrome
ODEs	Ordinary Differential Equations
SARS	Severe Acute Respiratory Syndrome
SARS-CoV-1	Severe Acute Respiratory Syndrome Coronavirus
WHO	World Health Organization
$\mathbb{R}^n$	Euclidean space of n-dimensions
$\mathbb{M}^{n \times n}$	Set of all $n \times n$ matrices
$L^2([t_0, t_1]; \mathbb{R}^m)$	Set of functions $f : [t_0, t_1] \longrightarrow \mathbb{R}^m$ such that $\int_{t_0}^{t_1} |f|^2 < \infty$
$C([t_0, t_1]; \mathbb{R}^m)$	Set of functions $f : [t_0, t_1] \longrightarrow \mathbb{R}^m$ such that f is continuous
$\mathscr{R}_0$	Basic Reproduction Number

Chapter 1: Introduction

1.1 Description of Diabetes

Diabetes is a chronic disease characterized by high blood glucose levels resulting from the body's inability to produce insulin or insufficient insulin production. It can also be a result of the body's incapability of efficient insulin usage [1, 2]. In other words, Processes that can lead to the development of diabetes ranges from the destruction of the insulin producing beta cells in the pancreas by the immune system resulting in insulin deficiency to the abnormalities that results in insulin resistance [1].

1.2 Diabetes Complications

People with diabetes are at high risk of developing some long-term complications resulting from the prolonged periods of high blood glucose. These complications can effect different body organs including the eyes, kidneys, nerves, heart, blood vessels, and limbs [1, 3]. Possible eye complications resulting from diabetes includes blurring, cataracts, and blindness. Cataracts for instance is caused by glucose accumulation in the lenses of the eyes which eventually obstructs light transmission to the back of the eye causing the lenses to be opaque [3]. Since Kidneys are responsible for filtering blood, kidney damage might also be accompanied with diabetes. This is caused by filtering blood with high glucose levels which in turn damages the tiny blood vessels in the kidneys [3]. Other diabetes complications includes nerve damage, limb amputation, stroke, cardiovascular diseases and high blood pressure [3]. These complications could be avoided if diabetes is properly managed and dealt with [2]. Figure 1.1 illustrates possible diabetes complications on the different body parts.
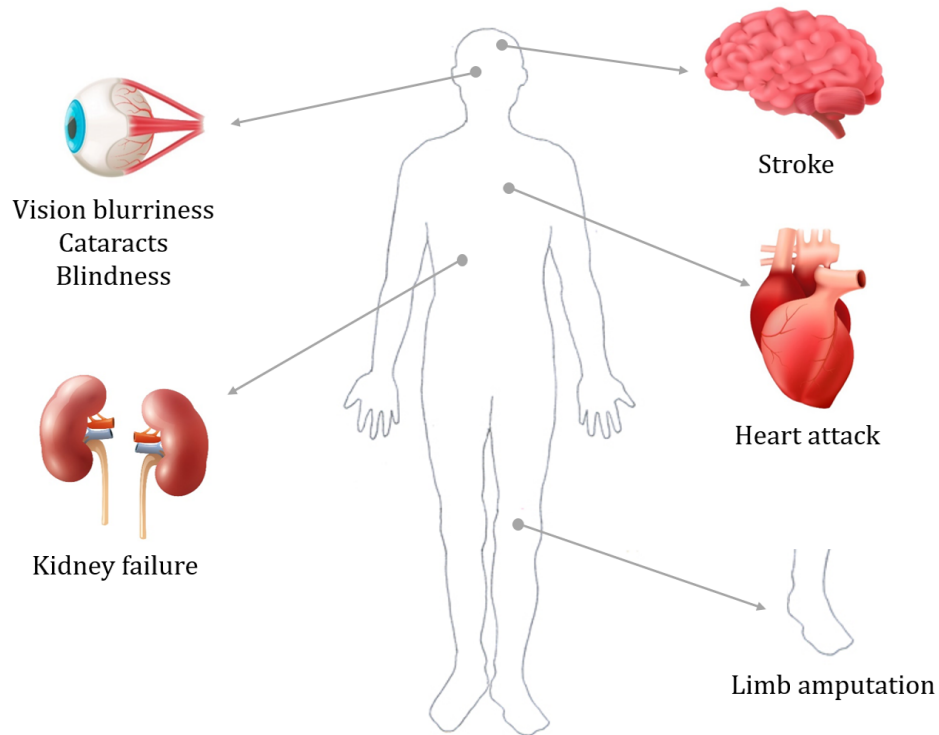
Figure 1.1: Diabetes complications

1.3 Types of Diabetes

Diabetes is commonly categorized into type 1 and type 2 diabetes. Type 1 diabetes is an autoimmune disease in which the immune system of the body attacks the beta cells that produces insulin leading to insufficient or no insulin production. On the other hand, type 2 diabetes is a result of what is known as insulin resistance, where the body cells are unable to fully react to insulin. Insulin is ineffective during the insulin resistance state. As a result, insulin is overly produced and over time the beta cells of the pancreas fails to keep up with the demand resulting in insufficient insulin production [1, 2]. Type 2 diabetes is more common as it accounts for 90% of diabetes cases [2].

1.4   Glucose-Insulin Regulatory System

The normal blood glucose concentration is within the range 70 – 110 mg/dl. The insulin and glucagon hormones which are secreted from the pancreatic beta and alpha cells respectively are responsible for maintaining blood glucose homeostasis as presented in Figure 1.2 [4]. Insulin hormone is released when the blood glucose concertation is high stimulating excess glucose uptake by the muscle, fat and liver cells and restraining hepatic glucose production which results in lowering the blood glucose concertation. On the other hand, glucagon hormone is released when the blood glucose concentration is low stimulating the conversion of the glycogen stored in the liver into glucose which results in increasing the blood glucose concentration [4].
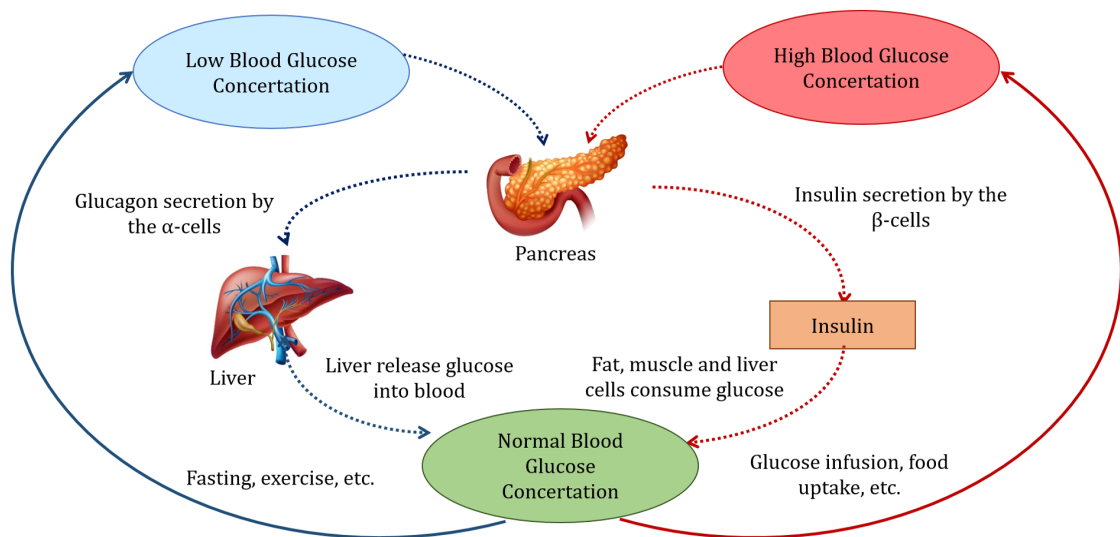
Figure 1.2: Blood glucose regulation

In case an individual's blood glucose concentration is continuously outside the normal range, then the individual is considered to have either hyperglycemia (glucose excess in bloodstream) or hypoglycemia (glucose deficiency in bloodstream). Diabetes mellitus is a disease characterized by hyperglycemia [4].

1.5   Prevalence of Diabetes

1.5.1   Worldwide

Diabetes is widely spread in the world given that the estimated number of the adult diabetic individuals aged 20 – 79 years worldwide was about 463 million in 2019 making up to 9.3% of the total adult population with type 2 accounting for nearly 90% of the diabetes cases. The number of diabetics is expected to increase to 578.4 million worldwide by 2030, in case the current trend continues [2]. Moreover, according to an estimate made in 2019 it was found that high-income countries have the highest prevalence of diabetes in adults of about 10.4% followed by middle-income countries with prevalence of 9.5%. On the other hand, low-income counties had the lowest prevalence of almost 4% [2].
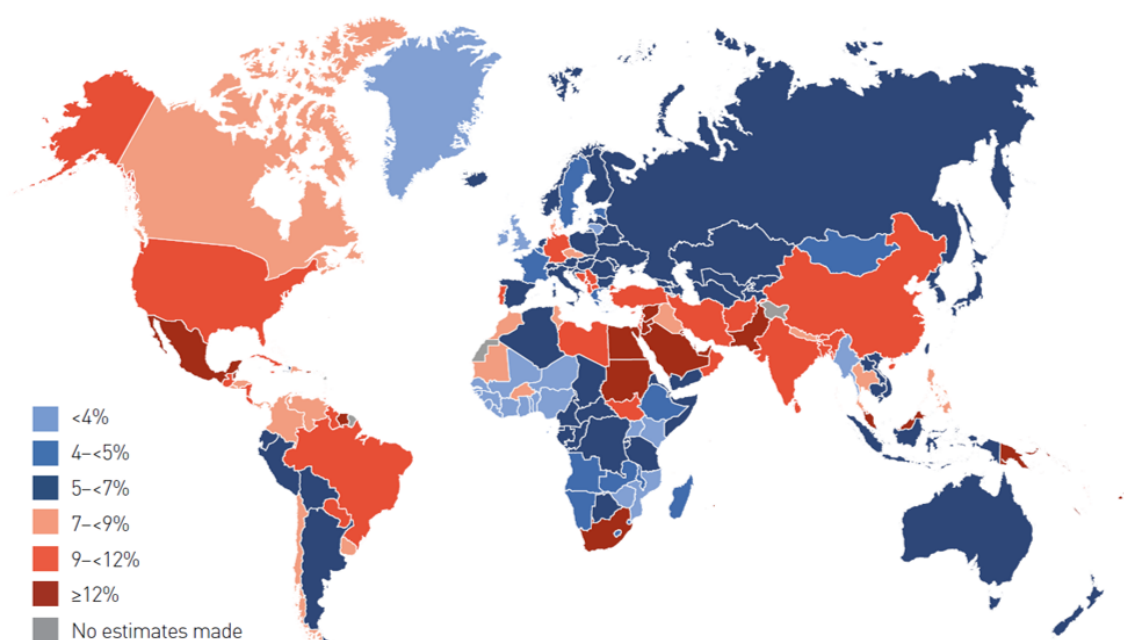
Figure 1.3: Estimated prevalence of diabetes in adults in 2019

Figure 1.3 (obtained from [2]) gives an illustration of the estimated prevalence of adults aged 20 – 79 years with type 1 and type 2 diagnosed and undiagnosed diabetes in the world map. Looking at the map one can clearly deduce that the Middle Eastern and North African regions are highly prevalent with diabetes.

1.5.2   MENA Region/Arab world

Diabetes is notably prevalent in the Middle Eastern and North African (MENA) region. In this region, it was estimated in 2019 that nearly 54.8 million adults aged 20 to 79 years have diabetes, which makes up to 12.8% of the total population. This prevalence percentage of 12.8% is considered the highest among the other world regions classified by the International Diabetes Federation (IDF) [2]. This region have the second-highest rate of increases in diabetes in the world [5].

There is a clear rise in type 2 diabetes mellitus in the Arab world of the MENA region. In fact, According to the IDF three Arab countries were among top ten countries in the prevalence of type 2 diabetes mellitus in 2013, namely, Saudi Arabia, Kuwait, and Qatar [5]. The high prevalence of type 2 diabetes mellitus in the Arab world can be a result of some risk factors that includes genetic factors which cannot be controlled and other modifiable risk factors such as obesity which is associated with eating habits and the lack of physical activity in addition to rapid urbanization [5]. Obesity is closely linked to type 2 diabetes as evidenced by many studies. For instance, a study was made in Kuwait with 1970 subjects of both genders found that 47.7% of obese males and 77.3% of obese females were diabetic [6]. Another study made in Saudi Arabia with 1385 male subjects found that 65% of diabetic patients were overweight [7]. Additionally, a study from Qatar of 1434 subjects found that 59.7% of diabetics were obese [8]. These studies serves as a great evidence of the correlation between type 2 diabetes and obesity.

Obesity is highly prevalent in the Arab world as evidenced by many studies and reports including a report made by the World Health Organization (WHO) in 2014 [9]. This report presented obesity percentages of adults in different countries of the world based on data from 2010. This report revealed that obesity is highly prevalent in Arab countries, especially in countries of the gulf region [9]. It stated that 55% and 30% of females and males respectively are obese in Kuwait. It also stated that 42% of females and 25% of males are obese in the UAE [9]. Since obesity is highly prevalent in the Arab world it would not be surprising for type 2 diabetes mellitus to be prevalent as well given

that the two are correlated.

The high incidence of obesity in the Arab world is mostly contributed by the followed dietary habits. This is pointed out by a study made on the dietary habits of some countries in the MENA region [10]. The analysis of this study suggested that many countries in the MENA region follow a diet that has low intake of fruits, vegetables and whole-grains and high intake of red and processed meats as well as foods high with sodium. Such dietary habits justifies weight gain and obesity [10]. Another factor that contributes to the spread of obesity in the Arab world is the inactive lifestyle that most Arabs adapt. This is demonstrated by a study made to assess physical activity in Arab countries [11]. This study concluded that the prevalence of physical inactivity exceeds 40% in almost every Arab country [11]. These factors that leads to obesity are usually associated with rapid urbanization as suggested by the prevalence rates of type 2 diabetes, where prevalence rates are much higher in urbanized countries compared to rural ones [5].

1.5.3   The United Arab Emirates

The United Arab Emirates has undergone a rapid development in the economy during the last two decades. This development had a positive influence in the country's educational and medical sectors. It has also led to increased prosperity. However, there is a downside to this development as there is a decrease in the physical activities as the lifestyle has become more sedentary. In addition, there is an increase in food intake along with bad dietary habits. These downsides has led to an increase in the prevalence of obesity together with type 2 diabetes mellitus [12]. In 2017, the IDF stated that the UAE is considered the second highest country in the percentage of age adjusted diabetes of adults in the MENA region with a percentage of 17.3% making up to 1185500 diabetes patients. The IDF also revealed that the number is expected to increase in case no intervention takes place [13].

1.6 Economical Facts of Diabetes Worldwide

Between direct medical costs of diabetes detection and treatment and indirect costs of absence or underperformance of diabetic workers, diabetes and its complications are a great burden to the national economies especially since diabetes complications are either long-term, severe or both [2, 4]. A study was made to estimate the global economic burden of diabetes in adults aged 20 – 79 years in 2015. In this study data were collected from 184 countries where direct diabetes costs were based on health expenditure data provided from the WHO and prevalence data provided from the IDF and indirect diabetes costs were estimated by assuming a human-capital approach were diabetes related morbidity and mortality were considered [14]. It was found that diabetes global economic burden accounts for about US$1.31 trillion with 34.7% credit to indirect costs [14].

1.7 COVID-19 and Diabetes

Corona Virus Disease 2019 (COVID-19) is a global viral disease that targets the respiratory system. What is concerning about this disease is that it is highly transmissible as it can be transmitted not only through direct contact of infected surfaces or droplets released from the infected, but it can also be transmitted through inhalation. The symptoms of this disease are mild for most patients, however, infected people with co-morbidities such as diabetes and cardiovascular diseases are at a higher risk of developing severe symptoms such as multi organ failure or even fatality [15]. A study of COVID-19 patients who were critically ill was carried out in Wuhan, china. Among 52 intensive care unit (ICU) patients it was found that 22% of 32 non survivors were diabetic [16]. Another study found that 12% among 120 critically ill COVID-19 patients were diabetic [16]. Furthermore, it has been evidenced that diabetic patients who were infected with any of the earlier corona viruses, namely, Severe Acute Respiratory Syndrome (SARS) or Middle East Respiratory Syndrome (MERS) had worse disease complications and higher mortality rates [17]. These studies suggests that having diabetes increases the severity of COVID-19 and its related fatality rates.

Chapter 2: Bergman's Minimal Model

2.1 The Origin of Bergman's Minimal Model

Over the years mathematical models have been used to describe the behavior of many different physiological systems. Many models were dedicated to investigate the blood glucose regulatory system in form of a system of differential equations, and these models varied from simple to complex [18]. Early models of the glucose-insulin dynamics were doubted and had a very limited role in the diagnosis and treatment of diabetes. This is caused by the unfamiliarity of using mathematical modeling to describe a closed-loop feedback physiological system [18]. Another reason was that organs which has a primary role in regulating the blood glucose concentration has non-linear functions by nature, given the fact that non-linear systems are unpredictable and difficult to solve [18, 19].

The characteristics of the beta cells, responsible for producing insulin, are considered complex, especially since it secretes insulin in two phases [18]. The first secretion phase starts after nutrient consumption and lasts for about 10 minutes, whilst the second phase is sustained until blood glucose concentration is within the normal range [20]. As a result, it is quite difficult to have a simple mathematical representation of the beta cells' function [18]. In order to overcome these complexities and efficiently use mathematical modeling to investigate the regulation of the blood glucose concentration, Bergman [21] utilized the Intravenous Glucose Tolerance Test (IVGTT) to form his model were he frequently measured plasma glucose and insulin of a group of test subjects following injecting them with a dose of glucose to see how plasma glucose interacts with insulin [18, 21].

The original purpose of the minimal model was to quantify the contribution of the responsivity of the beta cells to glucose (insulin secretion) and the sensitivity of the body tissues to the secreted insulin (insulin sensitivity) to the glucose tolerance. Where glucose tolerance can be defined as the body's ability to clear the blood from glucose [21].

2.2 The Intravenous Glucose Tolerance Test

The IVGTT is a clinical test that is used to determine the body's ability to metabolize glucose. At the beginning of this test venous fasting blood sample is obtained, thereafter, 25gm of glucose is injected intravenously during a period of two minutes, and within the next two hours samples of venous blood are continuously obtained and the last of which is used to decide whether the person has diabetes or not. That is if the blood glucose concentration is above 120 mg/dl, then the tested person has diabetes mellitus. Whereas if the blood glucose concentration is less than 100 mg/dl, then the tested person is most likely not diabetic. In case the glucose concentration lies in the range 100 − 120 mg/dl, then the test result is undefined [22].

2.3 Bergman's Minimal Model

Despite the existence of many models that describes the glucose-insulin dynamics, the Bergman minimal model is considered the simplest model that is useful and both efficient and accurate. This model is given by the following system of Ordinary Differential Equations (ODEs) [23]:

$$
\begin{aligned}
\dot{G} &= -p_1(G - G_b) - GX \\
\dot{X} &= -p_2 X + p_3(I - I_b) \\
\dot{I} &= -n(I - I_b) + \gamma[G - h]^+ t + u(t)
\end{aligned}
\tag{2.1}
$$

Where the state variables:

G: represents the plasma glucose concentration in $\frac{mg}{dl}$.

X: represents the effect of the active insulin on the glucose concentration in min^{-1}.

I: represents the plasma insulin concentration in $\frac{\mu U}{ml}$.

The constants G_b and I_b represents the basal values of the plasma glucose and insulin concentrations, and the Insulin infusion rate is represented by $u(t)$.

As for the parameters [23]:

p_1: is the insulin-dependent glucose disappearance rate in min^{-1}.

p_2 is the natural decrease rate of the ability of tissues to absorb glucose in min^{-1}.

p_3 is the insulin stimulated increase in tissue glucose absorption ability in $\left(min^{-2}\left(\frac{\mu U}{ml}\right)^{-1}\right)$.

Figure 2.1 and Figure 2.2 demonstrates the minimal model's glucose and insulin dynamics respectively:
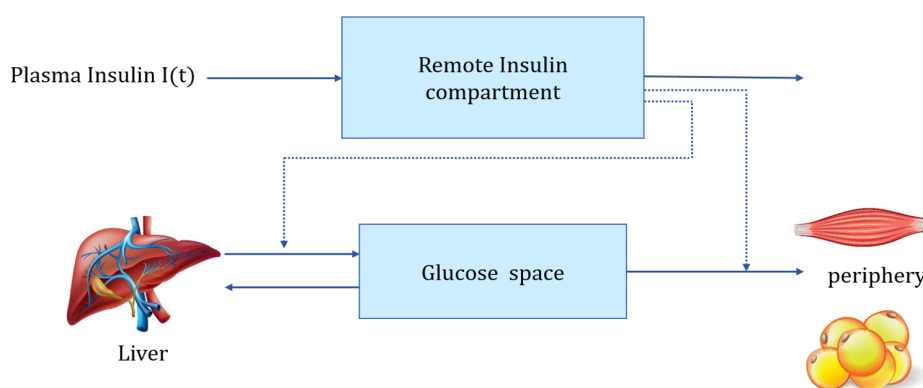
Figure 2.1: Minimal model of glucose disappearance
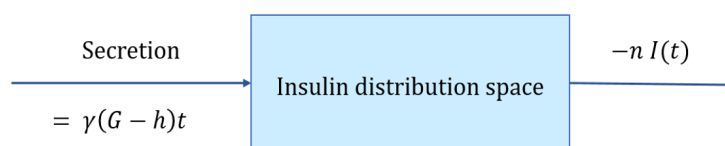
Figure 2.2: Minimal model of insulin kinetics

2.4 Cobeli's Model

A More comprehensive nonlinear model that includes the dynamics of the glucagon hormone is built by Cobelli [24]. This model is composed of three subsystems that describes the dynamics of the glucose, insulin and glucagon [24].

A single compartment is used in the glucose subsystem, this compartment describes the distribution and metabolism of glucose. It involves the balance of the liver's glucose pro-

duction and consumption, kidney's blood glucose filtration, the insulin dependent glucose utilization which is mainly done by the muscle and fat cells, in addition to the independent glucose utilization performed by the brain and nerve cells [24].

The insulin subsystem is composed of five compartments representing: insulin stored in the pancreas, instantly released pancreatic insulin, insulin in the plasma, insulin in the liver and insulin in the interstitial fluid (fluid presented in the small gaps between the body cells) [24, 25]. The glucagon subsystem is including a single compartment that involves the glucagon in the plasma and interstitial fluids [24].

The main purpose of this model was to investigate the interaction between glucose and insulin during the states of hyperglycemia. This model has been validated on both normal and pathological conditions, and it has been employed in researches that involves the regulation of carbohydrate metabolism [24].

2.5 More Extensions

Bergman's model has been widely used in the development of many blood glucose regulation models and other related applications. In fact, Bergman himself used his minimal model to develop a computer program that measures the insulin sensitivity, glucose effectiveness (glucose's own disappearance ability) along with the first and second phases of pancreatic responsivity [26].

Despite the usefulness and the many applications of Bergman's minimal model, it received many criticism [27]. The majorly criticized shortcomings of this model were the model's incoherence and lack of robustness in the procedure of parameter identification [27]. This is coming from the procedure that was performed to fit the model's parameters. The procedure was done in two steps. Firstly, recorded insulin concentration was regarded as an input to derive the glucose dynamics parameters. Secondly, recorded glucose concentration was regarded as an input to derive parameters of the insulin dynamics [28]. The two step parameter identification procedure decouples the glucose-insulin system even though, physiologically this system is a unified and an integrated feedback

system. Consequently, this is considered a limitation of Bergman's model [27, 28].

In order to overcome these shortcomings and furtherly improve the minimal model, many extended and modified versions of Bergman's model were proposed. One of those models [28] considered a single step parameter identification procedure and excluded the remote compartment presented in the minimal model resulting in a more coherent model. This model was also furtherly improved and modified.

Chapter 3: Literature Review - Mathematical Control Theory

3.1   Linear Control Systems

A linear control system can be described by the following system of ODEs [29, 30]:

$$\begin{cases} \dot{x} & = & A(t)x + B(t)u \\ x(t_0) & = & x_0 \end{cases} \tag{3.1}$$

Given the following assumptions:

1. $x(t) \in \mathbb{R}^n$, and is both real and continuous and satisfies equation (3.1).

2. $A(t) \in \mathbb{M}^{n \times n}$, $B(t) \in \mathbb{M}^{n \times m}$, and both of which are bounded and real.

3. In such a system, a controller $u(t) \in \mathbb{R}^m$ is selected so that it steers $x(t)$ from an initial state x_0 at t_0 to a desired state x_d at t_1. Given that $u(t)$ is real and bounded on the interval $[t_0, t_1]$ and assuming values from a non-empty set $\Omega \subseteq \mathbb{R}^m$.

The solution of such a linear system is given by [29]:

$$x(t) = \Phi(t)x_0 + \Phi(t) \int_{t_0}^{t} \Phi(s)^{-1} B(s)u(s)ds \tag{3.2}$$

Where $\Phi(t)$ is the fundamental matrix solution of the homogenous non-controlled linear system:

$$\dot{x} = A(t)x \tag{3.3}$$

In other words, $\Phi(t)$ is an $n \times n$ matrix whose columns are the linearly independent solutions of (3.3) with $\Phi(t_0) = I$. Moreover, if $A(t)$ is a constant A, then $\Phi(t) = e^{A(t-t_0)}$.

3.2 Autonomous Linear Control systems

Autonomous linear control systems are the ones in which the rate of change of the state variables with respect of time $\dot{x}$ does not depend explicitly on the time t.

Consider an autonomous linear control system with the following representation [29]:

$$\dot{x} = Ax + Bu \qquad (3.4)$$

In this system $x \in \mathbb{R}^n$. Matrix $A \in \mathbb{M}^{n \times n}$ and matrix $B \in \mathbb{M}^{n \times m}$, and both of which are real, constant valued matrices.

3.2.1 Controllability

In control theory, *Controllability* is regarded an essential attribute of a control system as it must be satisfied in order to achieve the desired controlling goal. The system defined by equation (3.4) with unrestrained control values (i.e. $u(t) \in \Omega = \mathbb{R}^m$) is said to be completely *controllable* in case for any two states x_0 , $x_1 \in \mathbb{R}^n$, there exists a controller $u(t)$ that steers x_0 to x_1 in a finite time [29, 30].

3.2.1.1 Controllability Test

Kalman's rank condition: One way to determine whether the linear system in hand is controllable or not is by finding the rank of the controllability matrix, which is an $n \times nm$ matrix of the following form [29, 30]:

$$C = [B, AB, A^2 B, ..., A^{n-1} B]$$

Then, the system is controllable if and only if $rank(C) = n$.

Controllability operator: Another method to check the controllability of a linear control system defined on an interval $[t_0, t_1]$ is to check the range of its corresponding controllability operator G, then:

Linear control system is controllable $\Leftrightarrow Range(G) = \mathbb{R}^n$

Where the controllability operator for this control system

$$G : L^2(t_0, t_1; \mathbb{R}^m) \longrightarrow \mathbb{R}^n$$

is defined as follows,

$$G(u) = \int_{t_0}^{t_1} e^{A(t_1-s)} Bu(s)ds,$$

Other methods to test the controllability of an autonomous linear system are presented in [29] along with its proofs.

3.2.2 Observability

A control system is *observable* if observations or measurements of the output over a finite time interval provides enough information to determine the internal states of the system. In other words, if knowledge of the output $y(t)$ on any time interval $[t_0, t_1]$ allows the computation of the initial state of the system $x(t_0) = x_0$, then the system is observable [29, 30].

The observability equation for the linear system in (3.4) is given by [29, 30]:

$$y(t) = Hx(t) \tag{3.5}$$

Where $y(t) \in \mathbb{R}^r$ represents the observable output, and $H \in \mathbb{M}^{r \times n}$ is a real constant matrix.

3.2.2.1 Observability Test

Kalman's rank condition: Determining whether the linear system defined by equations (3.4) and (3.5) is observable or not can be done using the Observability matrix which

is an $rn \times n$ matrix with the following form [29, 30]:

$$O = \begin{bmatrix} H \\ HA \\ HA^2 \\ \vdots \\ HA^{n-1} \end{bmatrix}$$

Then, the system is observable if and only if $rank(O) = n$.

Observability operator: Another possible way to check the observability of a linear control system defined on an interval $[t_0, t_1]$ is to check the observability operator μ, where

Linear control system is observable $\Leftrightarrow$ μ is one-to-one.

Where the observability operator for this control system

$$\mu : \mathbb{R}^n \longrightarrow L^2(t_0, t_1; \mathbb{R}^r)$$

is defined as follows,

$$\mu(z) = He^{A(\cdot)}z$$

Other methods to test the observability of an autonomous linear control system are presented in [29] along with its proofs.

3.2.3 The Duality Property

Observability and controllability are related in linear systems as they have a duality between them as proposed by the following theorem [29]:

Theorem 3.2.1. *The autonomous linear observed control system given by*

$$\dot{x} = Ax + Bu, \qquad y(t) = Hx \tag{3.6}$$

is observable if and only if the dual system given by

$$\dot{x} = A^T x + H^T u, \qquad y(t) = B^T x \tag{3.7}$$

is controllable.

To test the validity of theorem (3.2.1), it is assumed that the system defined by (3.6) is observable, then:

$$rank \begin{bmatrix} H \\ HA \\ HA^2 \\ \vdots \\ HA^{n-1} \end{bmatrix} = n$$

Since the transpose of any matrix has the same rank as the original one then,

$$rank \begin{bmatrix} H^T, & A^T H^T, & \dots & ,(A^T)^{n-1} H^T \end{bmatrix} = n$$

Which applies that a linear system defined by (3.7) is controllable and vice versa.

3.3 Optimal Trajectory Tracking

Trajectory tracking aims to lead the state trajectories $x(t) \in \mathbb{R}^n$ of a dynamical system to track a desired reference trajectory $x_d(t) \in \mathbb{R}^n$ that is defined over an interval $[t_0, t_1]$. In this case, the closer $x(t)$ is to $x_d(t)$ the better the controlling goal is achieved. Ideally, $x(t) = x_d(t)$ at all times $t > 0$ [31].

A suitable measure of the distance between $x(t)$ and $x_d(t)$ is provided by the following

equation [31]:

$$\mathscr{J}[x(t)] = \frac{1}{2} \int_{t_0}^{t_1} ((x(t) - x_d(t))^2 dt \tag{3.8}$$

Optimal trajectory tracking aims to minimize the distance between $x(t)$ and $x_d(t)$. This is done by finding a control $u(t) \in \mathbb{R}^m$ that minimizes $\mathscr{J}[x(t)]$ such that other controllers results in larger distances between $x(t)$ and $x_d(t)$.

Equation (3.8) might lead to an ill-defined $u(t)$ and $x(t)$ functions, so a possible way to fix this problem is by adding an additional regularization term as provided by the following equation [31]:

$$\mathscr{J}[x(t), u(t)] = \frac{1}{2} \int_{t_0}^{t_1} ((x(t) - x_d(t))^2 dt + \frac{\varepsilon^2}{2} \int_{t_0}^{t_1} |u(t)|^2 dt \tag{3.9}$$

The additional term in (3.9) ensures a well defined solution and avoids large controls. However, in most biological control systems the control $u(t) \in \Omega$ where Ω is a restrained subset of $\mathbb{R}^m$. This restrain depends on the biological nature of the control. Therefore, the additional term in equation (3.9) is removed and the equation is reduced back to equation (3.8) since the main goal of the control system in this case is to track x_d.

3.4 Semilinear Control Systems

A semilinear control system can be described by the following system of ODEs [32]:

$$\begin{cases} \dot{x} &= A(t)x(t) + B(t)u(t) + f(t, x(t), u(t)) \quad ,t \in (t_0, t_1] \\ x(t_0) &= x_0 \end{cases} \tag{3.10}$$

Given the following assumptions:

1. $x(t) \in \mathbb{R}^n$, $u(t) \in \mathbb{R}^m$.

2. $A(t)$ and $B(t)$ are continuous real matrices with $A(t) \in \mathbb{M}^{n \times n}$ and $B(t) \in \mathbb{M}^{n \times m}$.

3. $u(t) \in L^2([t_0, t_1]; \mathbb{R}^m)$.

4. $f : [t_0, t_1] \times \mathbb{R}^n \times \mathbb{R}^m \to \mathbb{R}^n$ is continuous.

3.4.1 Approximate Controllability of a Semilinear System

Definition 3.4.1. The semilinear system (3.10) is said to be *approximately controllable* on an interval $[t_0, t_1]$, if for any $\varepsilon > 0$, initial state $x_0 \in \mathbb{R}^n$, and final state $x_1 \in \mathbb{R}^n$ there exists a control $u \in C([t_0, t_1]; \mathbb{R}^m)$ such that the corresponding solution of system (3.10) satisfies the following condition [33]:

$$\|x(t_1) - x_1\| < \varepsilon$$

3.4.2 Exact Controllability of a Semilinear System

Definition 3.4.2. The semilinear system (3.10) is said to be *exactly controllable* on an interval $[t_0, t_1]$ if for any initial and final states $x_0, x_1 \in \mathbb{R}^n$, there exists a control $u \in C([t_0, t_1]; \mathbb{R}^m)$ such that the corresponding solution of system (3.10) satisfies [33]:

$$x(t_0) = x_0, \qquad x(t_1) = x_1$$

3.4.3 Observability of a Semilinear System

Definition 3.4.3. A semilinear system of the form (3.10) along with an observation:

$$y = Hx$$

is said to be *observable* on an interval $[t_0, t_1]$, if any pair of observation and control (y, u) uniquely determines the initial condition of the system. In other words, for two solutions

of (3.10) $x_1(t)$ and $x_2(t)$, if

$$Hx_1(t) = Hx_2(t), \quad \forall t \in [t_0, t_1]$$

then,

$$x_1(t_0) = x_2(t_0)$$

Chapter 4: Artificial Pancreas and Diabetes

4.1   Problem Statement

As stated in Chapter 1, the normal fasting blood glucose concentration ranges between 70 mg/dl to 110 mg/dl. People with type 1 or type 2 diabetes have blood glucose concentrations that exceeds the normal range for prolonged periods of time. A possible way to manage diabetes mellitus, especially type 1 is the *artificial pancreas*, which is a closed-loop control system that regulates the patient's blood glucose level. This system consists of a continuous blood glucose monitoring sensor (CGM), a control algorithm and an external insulin pump [34]. The CGM measures the patient's blood glucose level and sends the measurement to a small computer that acts as a moderator between the CGM and the insulin pump. This computer then calculates the required amount of insulin to maintain the blood glucose concentration within the normal range based on a built-in control algorithm. Followingly, the computer sends a signal of the calculated amount to the external insulin pump to inject the patient with the calculated amount. This way the artificial pancreas imitates the function of a healthy individual's pancreas. Figure 4.1 shows a block diagram of the function of an artificial pancreas.
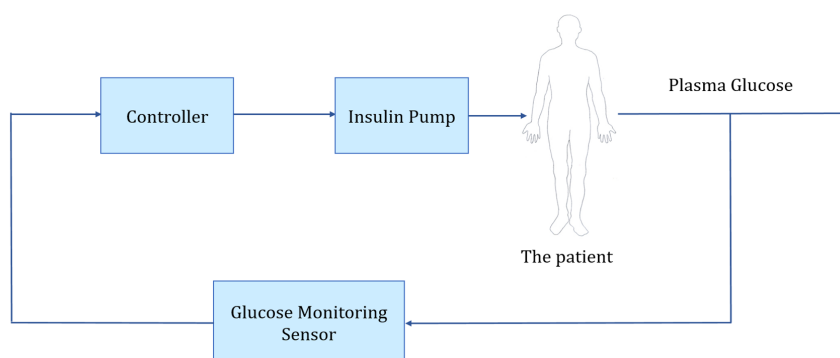
Figure 4.1: Block diagram of an artificial pancreas

A mathematical model of the blood glucose regulatory system is required to integrate the CGM to the insulin pump in an artificial pancreas. Furthermore, since the artificial pancreas is a control system, where the controlled variable is the blood glucose concentration and the control input is the external insulin infused through the pump. then, the patient's blood glucose concentration can only be regulated when the artificial pancreas is both controllable and observable. The aim of this part of the thesis is to prove both the controllability and observability of an existing artificial pancreas control design.

4.2 Existing Approach

An existing feedback and feedforward controller design for an artificial pancreas is presented in [35]. In this design the mathematical model used to describe the dynamics of the plasma insulin and glucose is the Bergman's minimal model. Since the parameters of the model differ slightly amongst people, the model was slightly altered to include parameter uncertainties so that the artifical pancreas can be tailored to fit a wide range of people [35].

In [35] an exogenous glucose input J from food that passes through the intestines is included. Moreover, it is assumed that the reference/desired glucose R as well as the exogenous glucose J are time-varying. Furthermore, the designed controller is both feedback and feedforward. The feedback part uses the actual blood glucose concentration G as an output whereas, the exogenous glucose J and the desired glucose R are regarded as disturbances for the feedforward part. Then, the controller $u = u(G, R, J)$ is designed such that it tracks the desired glucose for any slight parameter variations. The flow diagram of the feedback and feedforward controller is presented in Figure 4.2.

The version of the minimal model that has been used in [35] without parameter uncertain-
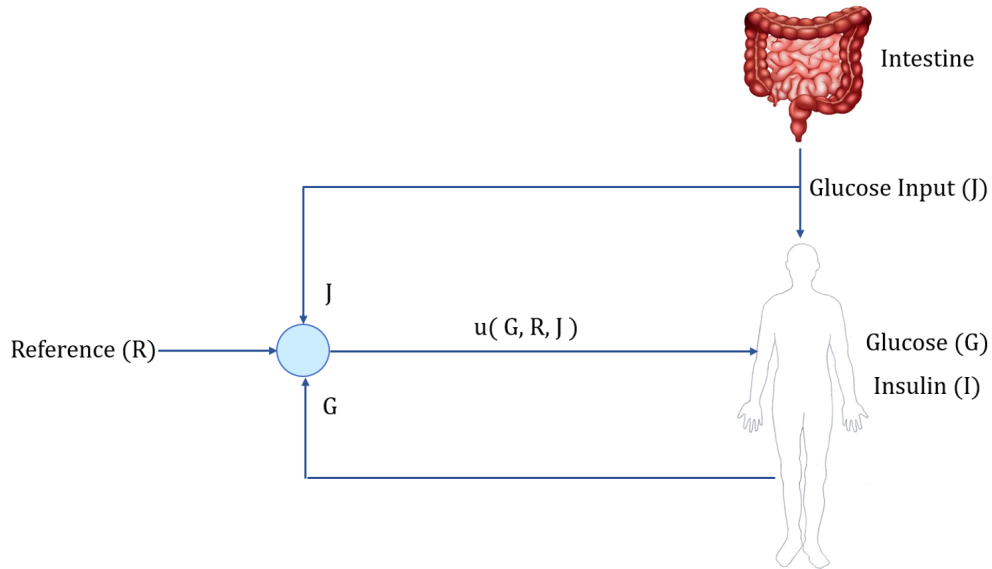
Figure 4.2: Flow diagram of feedback and feedforward controller

ties is described by the following nonlinear system of ODEs:

$$
\begin{cases}
\frac{dG}{dt} &= -m_1 G - XG + J \\[2mm]
\frac{dX}{dt} &= -m_2 X + m_3 I \qquad (4.1) \\[2mm]
\frac{dI}{dt} &= -m_4 I + u
\end{cases}
$$

Designing the controller involved using several mathematical tools including the Fourier series polynomials, the center manifold theory, variable transformations and more. to learn more check the main reference [35].

4.2.1 Results and Problems of Approach

The main aim of [35] was to design a feedback and feedforward controller $u = u(G, R, J)$ such that the actual blood glucose concentration G which is the controlled variable tracks a desired time varying glucose reference R while tolerating small parameter variations.

4.2.1.1 Results

In order to test the efficiency of the designed controller, numerical simulations were performed using a 24 hour insulin and glucose profiles of a group of normal men obtained from the experiment published in [36]. The simulated controlled glucose concentration G and the tracked glucose reference R obtained from [36] are plotted together in the following figure (obtained from [35]).
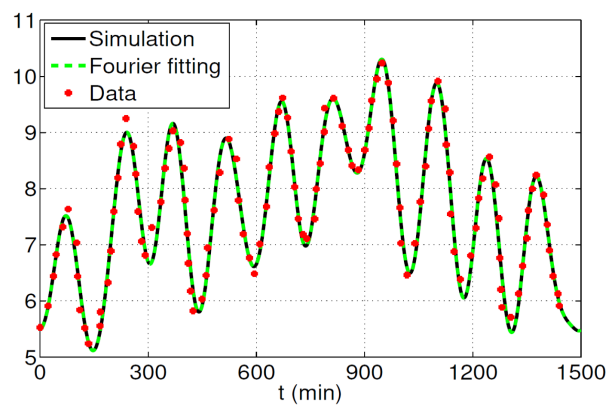
Figure 4.3: Glucose tracking under robust controller

Figure 4.3 shows that the designed controller succeeded in achieving its goal since clearly the controlled glucose concentration asymptotically tracks the reference glucose.

4.2.1.2 Problems

Even though the tracking goal of the controller in [35] was achieved, a problem rise in the mathematical formulation of the tracking goal. That is,

$$\lim_{t \to \infty} (G(t) - R(t)) = 0$$

The problem with this formulation is that the time t that is needed for G to track R could range from a couple of hours to a few days or even weeks. In other words, there is

no time restriction, which is a problem considering that this is a biological problem that involves a diabetic patient. The issue here is that it might take days before G could track R. Accordingly, G could have a very high oscillations that can damage the patient's organs and cause him some serious health issues that could eventually lead to the development of some long term complications. Moreover, many diabetics turn off their artificial pancreas when sleeping, which furtherly emphasize the importance of having an appropriate working time frame for the artificial pancreas. As a result, this approach is not practical. Therefore, it is better to consider a more realistic approach when addressing the issue of blood glucose regulation. Moreover, the controllability and observability of the artificial pancreas where not checked even though it is an essential step in control design.

4.2.2 Contribution of Thesis and Possible Future Work

Firstly, since [35] did not include any controllability or observability proofs. The first part of this thesis is dedicated to prove the controllability and the observability of the Bergman model presented in [35] without the inclusion of the parameter uncertainties.

Secondly, a possible future work that could improve what was made in [35] is to find an optimal control u such that the output $G(t) = R(t)$ at all times $t > 0$. Achieving this goal seems possible using the *Trajectory Controllability* approach which is also known as *T-Controllability* were the aim is to look for a controller that steers the state variable trajectories of a system along a specified trajectory instead of steering the state variables from an initial state to a desired final one [37].

4.3 Proofs of the Controllability and the Observability

In the presented proofs it is assumed that the exogenous glucose input J in system (4.1) is also a control variable in addition to u. This assumption was based on the fact that the glucose input can be controlled through the management of the dietary habits. Therefore, the control of system (4.1) is going to have the following form:

$$v = \begin{pmatrix} J \\ u \end{pmatrix}$$

Then, model (4.1) can be presented in the following semilinear form:

$$\dot{z}(t) = Az(t) + Bv(t) + F(z), \quad t \geq 0 \tag{4.2}$$

Along with the observation

$$y = Hz \tag{4.3}$$

Where,

$$z = \begin{pmatrix} G \\ X \\ I \end{pmatrix}, \quad A = \begin{pmatrix} -m_1 & 0 & 0 \\ 0 & -m_2 & m_3 \\ 0 & 0 & -m_4 \end{pmatrix}, \quad B = \begin{pmatrix} 1 & 0 \\ 0 & 0 \\ 0 & 1 \end{pmatrix}$$

Since the output/measure is G, then

$$H = \begin{pmatrix} 1 & 0 & 0 \\ 0 & 0 & 0 \\ 0 & 0 & 0 \end{pmatrix}$$

Before looking into the controllability of system (4.2), it is necessary to study the control-

lability of the corresponding linear system of ODEs:

$$
\begin{aligned}
\dot{z}(t) &= Az(t) + Bv(t), \quad t \in (t_0, \tau] \\
z(t_0) &= z_0
\end{aligned}
$$
(4.4)

Proposition 4.3.1. *System (4.4) is exactly controllable on any interval $[t_0, \tau]$, with $t_0 < \tau$.*

Proof. The proof is straightforward using Kalman's rank [29, 30] condition. i.e.,

$$Rank[B|AB|A^2B] = 3$$

In fact,

$$
AB = \begin{pmatrix} -m_1 & 0 & 0 \\ 0 & -m_2 & m_3 \\ 0 & 0 & -m_4 \end{pmatrix} \begin{pmatrix} 1 & 0 \\ 0 & 0 \\ 0 & 1 \end{pmatrix} = \begin{pmatrix} -m_1 & 0 \\ 0 & m_3 \\ 0 & -m_4 \end{pmatrix}
$$

And,

$$
A^2B = \begin{pmatrix} m_1^2 & 0 & 0 \\ 0 & m_2^2 & -m_3(m_2+m_4) \\ 0 & 0 & m_4^2 \end{pmatrix} \begin{pmatrix} 1 & 0 \\ 0 & 0 \\ 0 & 1 \end{pmatrix} = \begin{pmatrix} m_1^2 & 0 \\ 0 & -m_3(m_2+m_4) \\ 0 & m_4^2 \end{pmatrix}
$$

Hence, the controllability matrix C is given by the following 3×6 matrix:

$$
C = \begin{bmatrix} B & \vdots & AB & \vdots & A^2B \end{bmatrix} = \begin{bmatrix} 1 & 0 & \vdots & -m1 & 0 & \vdots & m_1^2 & 0 \\ 0 & 0 & \vdots & 0 & m_3 & \vdots & 0 & -m_3(m_2+m_4) \\ 0 & 1 & \vdots & 0 & -m_4 & \vdots & 0 & m_4^2 \end{bmatrix}
$$

And by reducing matrix C, it is found that $Rank(C) = 3 \implies$ the linear system (4.4) is controllable on any time interval $[t_0, \tau]$, with $t_0 < \tau$.

4.3.1 Approximate Controllability

In order to help prove the approximate controllability of system (4.2) a time delay of r is introduced in the term of non-linearity to get the following system:

$$
\begin{aligned}
\frac{dG}{dt} &= -m_1 G + J - X(t-r)G(t-r) \\
\frac{dX}{dt} &= -m_2 X + m_3 I \\
\frac{dI}{dt} &= -m_4 I + u
\end{aligned}
\tag{4.5}
$$

Along with the following initial conditions:

$$
\begin{aligned}
G(s) &= \phi_1(s), \quad s \in [-r,0] \\
X(s) &= \phi_2(s), \quad s \in [-r,0] \\
I(s) &= \phi_3(s), \quad s \in [-r,0]
\end{aligned}
$$

Where $\phi_1(s)$, $\phi_2(s)$ and $\phi_3(s)$ are functions of the historical data of each state variable.

System (4.5) along with its initial conditions can be represented compactly as follows:

$$
\begin{aligned}
\dot{z}(t) &= Az(t) + Bv(t) + F(z_t(-r)), \quad t \geq 0 \\
z(s) &= \phi(s), \quad s \in [-r,0]
\end{aligned}
\tag{4.6}
$$

where the function $z_t \colon [-r,0] \to \mathbb{R}^3$ is defined by:

$$
z_t(s) = z(t+s)
$$

Definition 4.3.1. System (4.6) is said to be approximately controllable on an interval $[0, \tau]$ if for any $\varepsilon > 0$, $\phi \in C([-r, 0]; \mathbb{R}^3)$ and final state $z_1 \in \mathbb{R}^3$ there exists a control $v \in C([0, \tau]; \mathbb{R}^2)$ such that the corresponding solution of system (4.6) satisfies two conditions:

1. $z(0) = \phi(0)$

2. $\|z(\tau) - z_1\| < \varepsilon$

In this case the solution of (4.6) is given by:

$$
\begin{aligned}
z(t) &= e^{At}\phi(0) + \int_0^t e^{A(t-s)}Bv(s)ds + \int_0^t e^{A(t-s)}f(z_s(-r))ds, \quad t \in [0, \tau] \\
z(s) &= \phi(s), \quad\quad\quad\quad\quad\quad\quad\quad\quad\quad\quad\quad\quad\quad\quad\quad\quad\quad\quad\quad s \in [-r, 0]
\end{aligned}
$$

To assist proving the approximate controllability of system (4.6), the Gramian matrix of the linear system (4.4) must be defined. Where the Gramian matrix definition is given by:

Definition 4.3.2. Given a set of vectors v_1, v_2,...,v_n. The *Gramian matrix* or the *Gram matrix* $G = [g_{ij}] \in \mathbb{C}^{n \times n}$ of these vectors is defined by [38]:

$$
g_{ij} = \langle v_i, v_j \rangle, \quad\quad i, j \in 1, 2, ..., n
$$

The Gramian matrix/operator of the linear system (4.4) is given by:

$$
W_{t_0} = \int_{t_0}^{\tau} e^{A(\tau-s)}BB^T e^{A^T(\tau-s)}ds
$$

The solution of system (4.4) at any time $t = \tau$ with initial condition $z(t_0) = z_0$ is given by:

$$
z(\tau) = e^{A\tau}z_0 + \int_{t_0}^{\tau} e^{A(\tau-s)}Bv_{t_0}(s)ds
$$

Consequently, a control v_{t_0} steering system (4.4), from an initial state z_0 to a final state z_1 is given by:

$$v_{t_0}(t) = B^T e^{A^T(\tau-t)} W_{t_0}^{-1}(z_1 - e^{A\tau}z_0), \quad \forall t \in [t_0, \tau]$$

As shown by,

$$
\begin{aligned}
z(\tau) &= e^{A\tau}z_0 + \int_{t_0}^{\tau} e^{A(\tau-s)}BB^T e^{A^T(\tau-s)} W_{t_0}^{-1}(z_1 - e^{A\tau}z_0) \, ds \\
&= e^{A\tau}z_0 + \int_{t_0}^{\tau} e^{A(\tau-s)}BB^T e^{A^T(\tau-s)} \, ds \ W_{t_0}^{-1}(z_1 - e^{A\tau}z_0) \\
&= e^{A\tau}z_0 + W_{t_0} W_{t_0}^{-1}(z_1 - e^{A\tau}z_0) \\
&= e^{A\tau}z_0 + z_1 - e^{A\tau}z_0 \\
&= z_1
\end{aligned}
$$

After defining the approximate controllability of system (4.6) and the Gramian of the linear system (4.4) the proof can be done.

Theorem 4.3.2. *The semilinear system with delay (4.6) is approximately controllable on* $[0, \tau]$.

Proof. For a given $\phi \in C([-r, 0]; \mathbb{R}^3)$, a final state z_1 and $\varepsilon > 0$, it is required to find a controller $v \in C([0, \tau]; \mathbb{R}^2)$ such that the corresponding solution $z_v(.)$ of (4.6) satisfies:

$$\|z(\tau) - z_1\| < \varepsilon$$

A fixed control $v \in C([0, \tau]; \mathbb{R}^2)$ is considered with a corresponding solution $z(t, \phi, v) = z(t)$. Then, a number δ is considered such that is small enough so that $\delta < r < \tau$ and the

control is defined by:

$$v_\delta(t) = \begin{cases} v(t), & if \quad 0 < t < \tau - \delta \\ \\ v_{\tau-\delta}(t), & if \quad \tau - \delta < t \leq \tau \end{cases}$$

where,

$$v_{\tau-\delta}(t) \;\; = \;\; B^T e^{A^T(\tau-t)} W_{\tau-\delta}^{-1}(z_1 - e^{A\tau}z(\tau-\delta)), \qquad \tau - \delta \leq t \leq \tau$$

The solution of (4.6) corresponding to the control $v_\delta(t)$ denoted by $z^\delta(t)$ is given by:

$$z^\delta(t) = e^{At}\phi(0) + \int_0^t e^{A(t-s)} B v_\delta(s) ds + \int_0^t e^{A(t-s)} F(z_s^\delta(-r)) ds$$

Evaluating $z^\delta(t)$ at $t = \tau$ and taking $e^{A\delta}$ as a common factor, the following is obtained:

$$\begin{aligned} z^\delta(\tau) \;\; = \;\; & e^{A\delta}\left\{ e^{A(\tau-\delta)}\phi(0) + \int_0^{\tau-\delta} e^{A(\tau-\delta-s)} B v(s) ds + \int_0^{\tau-\delta} e^{A(\tau-\delta-s)} F(z_s^\delta(-r)) ds \right\} \\ & + \;\; \int_{\tau-\delta}^\tau e^{A(\tau-s)} B v_{\tau-\delta}(s) ds + \int_{\tau-\delta}^\tau e^{A(\tau-s)} F(z_s^\delta(-r)) ds \end{aligned}$$

The expression is simplified to get:

$$\begin{aligned} z^\delta(\tau) \;\; = \;\; & e^{A\delta}z^\delta(\tau-\delta) + \int_{\tau-\delta}^\tau e^{A(\tau-s)} B v_{\tau-\delta}(s) ds + \int_{\tau-\delta}^\tau e^{A(\tau-s)} F(z_s^\delta(-r)) ds \\ \;\; = \;\; & z_1 + \int_{\tau-\delta}^\tau e^{A(\tau-s)} F(z_s^\delta(-r)) ds \end{aligned}$$

After moving z_1 to the other side, the expression can be represented by:

$$z^\delta(\tau) - z_1 = \int_{\tau-\delta}^\tau e^{A(\tau-s)} F(z_s^\delta(-r)) ds$$

Then, by taking the norm, the following inequality is obtained:

$$\left\| z^{\delta}(\tau) - z_1 \right\| \leq \int_{\tau-\delta}^{\tau} \left\| e^{A(\tau-s)} \right\| \left\| F(z^{\delta}(s-r) \right\| ds \leq \int_{\tau-\delta}^{\tau} M \left\| F(z^{\delta}(s-r)) \right\| ds$$

Since $z^{\delta}(s-r) = z(s-r)$, if $\tau - \delta \leq s \leq \tau$, then

$$\left\| z^{\delta}(\tau) - z_1 \right\| \leq \int_{\tau-\delta}^{\tau} M \left\| F(z(s-r)) \right\| ds$$

Take $K = \max_{s \in [0,\tau]} \left\{ \left\| e^{A(\tau-s)} \right\| \left\| F(z(s-r)) \right\| \right\}$ and $\delta < \min \left\{ r, \frac{\varepsilon}{K} \right\}$ to get:

$$\left\| z^{\delta}(\tau) - z_1 \right\| < \varepsilon$$

4.3.2 Exact Controllability

The exact controllability of system (4.2) is going to be proved without the inclusion of a time delay. However, it will still involve a slight modification in the system. The proof employs the *Banach contraction mapping theorem* which is also known as the *Banach fixed point theorem* which has the following definition:

Definition 4.3.3. Let X be a complete metric space and $T : X \longrightarrow X$ be a contraction map, meaning, there exists a constant $q \in (0,1)$ such that $d(T(x), T(y)) \leq qd(x,y)$ for all $x, y \in X$. Then, there exists a unique point z, such that $T(z) = z$. In other words, T has a fixed point [39].

System (4.2) can be written in the following slightly altered way:

$$
\begin{aligned}
\frac{dG}{dt} &= -m_1 G - m_5 X + X(m_5 - G) + J \\
\frac{dX}{dt} &= -m_2 X + m_3 I \\
\frac{dI}{dt} &= -m_4 I + u
\end{aligned}
\tag{4.7}
$$

With the initial conditions:

$$
\begin{aligned}
G(0) &= G_0 \\
X(0) &= X_0 \\
I(0) &= I_0
\end{aligned}
$$

Which can be presented in the following compact form:

$$
\begin{aligned}
\dot{z}(t) &= Az + Bv + F(z) \\
z(0) &= z_0
\end{aligned}
\tag{4.8}
$$

Where,

$$
z = \begin{pmatrix} G \\ X \\ I \end{pmatrix}, \quad
A = \begin{pmatrix} -m_1 & -m_5 & 0 \\ 0 & -m_2 & m_3 \\ 0 & 0 & -m_4 \end{pmatrix}, \quad
B = \begin{pmatrix} 1 & 0 \\ 0 & 0 \\ 0 & 1 \end{pmatrix}
$$

Before proving the exact controllability of system (4.8), it is favored to start by proving the following corresponding linear system:

$$
\dot{z}(t) = Az + Bv, \qquad t \in (0, \tau]
\tag{4.9}
$$

Proposition 4.3.3. *The linear system (4.9) associated with the semilinear system (4.8) is exactly controllable on the interval $[0, \tau]$.*

Proof. Just like the case of system (4.4), it would be enough to check the Kalman's rank condition [29, 30]:

$$AB = \begin{pmatrix} -m_1 & 0 \\ 0 & m_3 \\ 0 & -m_4 \end{pmatrix}, \quad A^2B = \begin{pmatrix} m_1^2 & -m_3m_5 \\ 0 & -m_3(m_2+m_4) \\ 0 & m_4^2 \end{pmatrix}$$

Then,

$$Rank\left[B|AB|A^2B\right] = Rank \begin{bmatrix} 1 & 0 & \vdots & -m_1 & 0 & \vdots & m_1^2 & -m_3m_5 \\ 0 & 0 & \vdots & 0 & m_3 & \vdots & 0 & -m_3(m_2+m_4) \\ 0 & 1 & \vdots & 0 & -m_4 & \vdots & 0 & m_4^2 \end{bmatrix} = 3$$

Hence, system (4.9) is exactly controllable on any time interval.

Before proving the exact controllability of system (4.8) the following operators of the corresponding linear system (4.9) needs to be defined:

○ The controllability operator $G : L^2(0,\tau;\mathbb{R}^2) \longrightarrow \mathbb{R}^3$ is defined by

$$G(v) = \int_0^\tau e^{A(\tau-s)}Bv(s)ds$$

○ The Gramian operator has the form

$$W = \int_0^\tau e^{A(\tau-s)}BB^T e^{A^T(\tau-s)}ds$$

○ The adjoint $G^* : \mathbb{R}^3 \to L^2(0,\tau;\mathbb{R}^2)$ is given by

$$(G^*(\zeta))(t) = B^T e^{A^T(\tau-t)}\zeta$$

It can be noted that the Gramian operator is a combination of the controllability operator G and its adjoint G^*, i.e.

$$W = GG^* = \int_0^\tau e^{A(\tau-s)}BB^T e^{A^T(\tau-s)}ds$$

Now, the exact controllability of system (4.8) can be proved.

Theorem 4.3.4. *Under some conditions the semilinear control system (4.8) is exactly controllable on the interval $[0, \tau]$.*

Proof. Firstly, system (4.8) is assumed to be exactly controllable on the interval $[0, \tau]$. Then, for any initial and final states $z_0, z_1 \in \mathbb{R}^3$, there exists a control $v \in C([0, \tau]; \mathbb{R}^2)$ such that the corresponding solution of (4.8) satisfies:

$$
\begin{aligned}
z_1 &= e^{A\tau} z_0 + \int_0^\tau e^{A(\tau - s)} Bv(s)ds + \int_0^\tau e^{A(\tau - s)} F(z(s))ds \\
&= e^{A\tau} z_0 + G(v) + \int_0^\tau e^{A(\tau - s)} F(z(s))ds
\end{aligned}
$$

Hence,

$$
G(v) = z_1 - e^{A\tau} z_0 - \int_0^\tau e^{A(\tau - s)} F(z(s))ds
$$

Now, v can be represented by the expression $v = G^* W^{-1} G(v)$ as shown by,

$$
\begin{aligned}
G(v) &= \int_0^\tau e^{A(\tau - s)} Bv(s)ds \\
G(v) &= \int_0^\tau e^{A(\tau - s)} BG^* W^{-1} G(v)ds \\
G(v) &= \int_0^\tau e^{A(\tau - s)} BB^T e^{A^T(\tau - s)} W^{-1} G(v)ds \\
G(v) &= \int_0^\tau e^{A(\tau - s)} BB^T e^{A^T(\tau - s)} ds W^{-1} G(v) \\
G(v) &= WW^{-1} G(v) \\
G(v) &= G(v)
\end{aligned}
$$

Therefore,

$$
v = G^* W^{-1} \left(z_1 - e^{A\tau} z_0 - \int_0^\tau e^{A(\tau - s)} F(z(s))ds \right)
$$

Now, an operator $\mathscr{L}$ is defined by:

$$
\begin{aligned}
\mathscr{L}(z) &= G^* W^{-1}\left(z_1 - e^{A\tau}z_0 - \int_0^\tau e^{A(\tau-s)}F(z(s))ds\right) \\
&= \Gamma\left(z_1 - e^{A\tau}z_0 - \int_0^\tau e^{A(\tau-s)}F(z(s))ds\right)
\end{aligned}
$$

Then, the solution of the initial value problem (4.8) can have the following representation:

$$
z(t) = e^{At}z_0 + \int_0^t e^{A(t-s)}B\mathscr{L}(z)(s)ds + \int_0^t e^{A(t-s)}F(z(s))ds
$$

Which motivates the definition of the following operator:

$$
\mathscr{P} : C([0,\tau];\mathbb{R}^3) \longrightarrow C([0,\tau];\mathbb{R}^3)
$$

That is defined by the following expression:

$$
(\mathscr{P}(z))(t) = e^{At}z_0 + \int_0^t e^{A(t-s)}B\mathscr{L}(z)(s)ds + \int_0^t e^{A(t-s)}F(z(s))ds
$$

Hence, the controllability problem is reduced to the problem of finding a fixed point for the operator $\mathscr{P}$, which can be done by proving that $\mathscr{P}$ is a contraction map. In fact,

$$
\begin{aligned}
(\mathscr{P}(z_2))(t) - (\mathscr{P}(z_1))(t) &= \int_0^t e^{A(t-s)}B(\mathscr{L}(z_2)(s) - \mathscr{L}(z_1)(s))ds \\
&+ \int_0^t e^{A(t-s)}(F(z_2(s)) - F(z_1(s)))ds
\end{aligned}
$$

By taking the norm and applying the triangular inequality, the following inequality is obtained:

$$
\begin{aligned}
\|(\mathscr{P}(z_2))(t) - (\mathscr{P}(z_1)(t))\| &\leq \int_0^t M \|\mathscr{L}(z_2)(s) - \mathscr{L}(z_1)(s)\| ds \\
&+ \int_0^t Mm_5 \|z_2(s) - z_1(s)\| ds
\end{aligned}
$$

Where

$$M = \max_{t \in [0,\tau]} \left\{ \left\| e^{At} \right\|, \left\| e^{At} B \right\| \right\},$$

The inequality $\| F(z_2) - F(z_1) \| \leq m_5 \| z_2(s) - z_1(s) \|$ can be proved directly by substituting the expression of $F(z)$. On the other hand,

$$\| \mathcal{L}(z_2)(s) - \mathcal{L}(z_1)(s) \| \quad \leq \| \Gamma \| \int_0^\tau M m_5 \| z_2(s) - z_1(s) \| \, ds$$

$$\leq \| \Gamma \| \tau M m_5 \| z_2 - z_1 \|$$

where,

$$\| \Gamma \| = \sup_{s \in [0,\tau]} \| B^T \| \left\| e^{A^T (\tau - s)} \right\| \| W^{-1} \| \leq \| B \| M \| W^{-1} \|$$

Hence,

$$\| \mathcal{L}(z_2)(s) - \mathcal{L}(z_1)(s) \| \leq \| B \| M^2 m_5 \| W^{-1} \| \tau (\| z_2 - z_1 \|)$$

Therefore,

$$\| \mathcal{P}(z_2) - \mathcal{P}(z_1) \| \leq (\| B \| M^3 \| W^{-1} \| m_5 \tau^2 + \tau m_5 M)(\| z_2 - z_1 \|)$$

$$\| \mathcal{P}(z_2) - \mathcal{P}(z_1) \| \leq (\| B \| M^2 \| W^{-1} \| \tau + 1) \tau m_5 M \| z_2 - z_1 \|$$

Consequently, $\mathcal{P}$ is contraction map in case the following condition holds:

$$(\| B \| M^2 \| W^{-1} \| \tau + 1) \tau m_5 M < 1$$

Accordingly, the following theorem is deduced:

Theorem 4.3.5. *System (4.8) is exactly controllable on the interval* $[0, \tau]$ *if the following*

condition holds

$$(\|B\| M^2 \|W^{-1}\| \tau + 1)\tau m_5 M < 1$$

where,

$$M = \max_{t \in [0,\tau]} \left\{ \left\| e^{At} \right\|, \left\| e^{At} B \right\| \right\}$$

and

$$W = \int_0^\tau e^{A(\tau-s)} BB^T e^{A^T(\tau-s)} ds$$

4.3.2.1   Example

To furtherly emphasize theorem (4.3.5), the following example is presented using parameter values obtained from the original paper [21] that presented bergman's model. In this example, the parameters are those of subject no.3 in [21]:

Parameter	Value
m_1	$0.0374\ min^{-1}$
m_2	$0.0478\ min^{-1}$
m_3	$0.00000873\ \frac{min^{-2}}{\left(\frac{\mu U}{ml}\right)}$
m_4	$0.3\ min^{-1}$

Then,

$$A = \begin{pmatrix} -0.0374 & -m_5 & 0 \\ 0 & -0.0478 & 0.00000873 \\ 0 & 0 & -0.3 \end{pmatrix} \quad B = \begin{pmatrix} 1 & 0 \\ 0 & 0 \\ 0 & 1 \end{pmatrix}$$

τ is arbitrarily set such that $\tau = 60$ *min* (1 hour), and $m_5 = 1.8 * 10^{-12}$ to get:

$$W = \begin{pmatrix} 13.2187 & -9.84478 * 10^{-29} & -1.2399 * 10^{-25} \\ -9.84478 * 10^{-29} & 7.60001 * 10^{-9} & 0.0000418344 \\ -1.2399 * 10^{-25} & 0.0000418344 & 1.66667 \end{pmatrix}$$

and

$$M = \max_{t \in [0,60]} \left\{ \left\| e^{At} \right\|, \left\| e^{At} B \right\| \right\} = 1$$

Then,

$$(\|B\|_{\infty} M^2 \|W^{-1}\|_{\infty} \tau + 1) \tau m_5 M = 0.989347 < 1$$

So, the inequality of Theorem (4.3.5) is satisfied. Therefore, system (4.8) in this case is exactly controllable on the time interval $[0, 60]$. Note that for the system to be exactly controllable, the value of m_5 should be selected based on the value of τ. For instance, in case $\tau = 60$ minutes then any positive value of m_5 such that $m_5 \leq 1.8 * 10^{-12}$ would satisfy the inequality. However, if the value of τ is increased to 120 minutes, then $m_5 = 1.8 * 10^{-12}$ would no longer satisfy the inequality and values of m_5 such that $m_5 \leq 4.5 * 10^{-13}$ would satisfy the inequality. Which means that in order to satisfy the inequality of Theorem (4.3.5) the value of m_5 should be decreased as the value of τ increases. Practically speaking, if the time τ to control the blood glucose level was to be increased, then the value of m_5 should be decreased, which implies that it would require more number of digits to be presented. This implies that the precision of the control system should increase to fit more number of digits as the controlling time increases. Hence, it would be preferred to use a high precision control system (artificial pancreas) when controlling a diabetic's blood glucose level.

4.3.3 Observability

Just like in the case of controllability. First, the observability of the linear system

corresponding to system (4.2) is proved. This linear system has the following form:

$$\dot{z} = Az + Bv \qquad (4.10)$$

$$y = Hz \qquad (4.11)$$

Then, the corresponding observability matrix is given by:

$$O = \begin{bmatrix} 1 & 0 & 0 \\ 0 & 0 & 0 \\ 0 & 0 & 0 \\ \dots & \dots & \dots \\ -m_1 & 0 & 0 \\ 0 & 0 & 0 \\ 0 & 0 & 0 \\ \dots & \dots & \dots \\ -m_1^2 & 0 & 0 \\ 0 & 0 & 0 \\ 0 & 0 & 0 \end{bmatrix}$$

$Rank(O) = 3 \longrightarrow$ system (4.10) is observable on any time interval according to Kalman's

Rank Condition [29, 30].

To prove the observability of the semilinear system (4.2), system (4.2) is considered to be

independent of the control variable, i.e.

$$\dot{z} = Az + F(z) \tag{4.12}$$

Then, the observability is proved directly using the following theorem from [40].

Theorem 4.3.6. *Assume that the transformations $f : \mathbb{R}^3 \longrightarrow \mathbb{R}^3$ and $h : \mathbb{R}^3 \longrightarrow \mathbb{R}^3$ to be continous. If the pair $(f_z(0), h_z(0))$ is observable, then the system (5.11) is observable at any time $t > 0$ [40].*

Where the transformations f and h are defined as follows:

$$
\begin{aligned}
f(z) &= Az + F(z) \\
h(z) &= Hz
\end{aligned}
$$

Then, $(f_z(0), h_z(0)) = (A, H)$. and since the linear system (4.10) is observable, then the semilinear system (4.2) - (4.3) is observable at any time $t > 0$, which is clearly true since the blood glucose level can be observed at any time through the CGM.

Chapter 5: Literature Review - Modeling of Infectious Diseases

5.1   Compartmental Disease Transmission Models

Mathematical modeling of infectious diseases is a powerful tool to study the spread of an infectious disease. These models can predict the progression of the disease spread, and they can also determine the key factors that contributes to the disease transmission making them a helpful tool in the development of the strategies that aids in the prevention and control of the disease spread [41].

These models are known as the Compartmental Disease Transmission Models. As the name suggests, in these models the population of concern is divided into compartments where each individual is characterized by a distinct state variable. In other words, no individual can be present in more than one compartment. A compartment can either be a disease compartment containing both symptomatically and asymptomatically infected individuals, or a non-disease compartment containing non diseased individuals [42].

In this case, the total population at issue is divided into n disease compartments and m non-disease compartments, then the disease transmission model can be written in the following form of a system of ODEs [42]:

$$\begin{aligned}
x'_i &= \mathscr{F}_i(x,y) - \mathscr{V}_i(x,y), & i = 1,2,...,n \\
y'_j &= \mathscr{G}_j(x,y), & j = 1,2,...,m
\end{aligned}$$

Where x_i, for $i \in 1,2,...,n$ represents a disease compartment, and y_j, for $j \in 1,2,...,m$ represents a non-disease compartment. Moreover, $\mathscr{F}_i$ represents the rate of increase of secondary infection in the disease compartment i, and $\mathscr{V}_i$ represents the rate of decrease

in the compartment *i* either by disease progression, recovery, or death.

5.2 SEIR Model

An example of a compartmental disease transmission model is the SEIR model. This model segregates the population of concern into four sub populations. Namely, susceptible or vulnerable population (S), Exposed or latent infected population (E), infectious population (I), and recovered population (R). This model assumes that all new infections takes place at the first stage when a susceptible individual comes into contact with an infected individual. SEIR models can be presented in may possible ways, one of which is written as follows [42]:

$$S' = \Pi - \mu S - \beta SI$$

$$E' = \beta SI - (\mu + \kappa)E$$

$$I' = \kappa E - (\mu + \alpha)I$$

$$R' = \alpha I - \mu R$$

Naturally, all initial conditions are non negative, since the number of individuals in a population cannot be negative. This representation assumes that the natural birth rate of susceptible persons is a constant Π. On the other hand, natural death rate is assumed to be μ for all the sub populations. The rate at which new infections emerges into the exposed sub population is βSI. Exposed individuals become infectious by the rate κ, and infected individuals recovers at the rate α.

It is to be noted that not all SEIR models have the presented form. Some of which neglects the natural birth and death rates. In addition, the presented model assumes that individuals gets immunity after recovery. However, some models assumes that the recovered individuals progresses to become susceptible again at a certain rate.

Figure 5.1 shows a flow chart of the presented SEIR model.
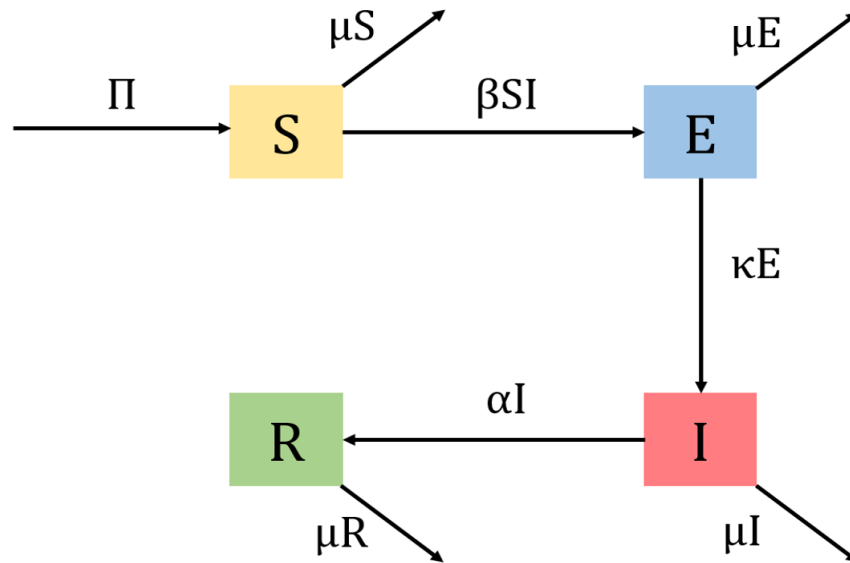
Figure 5.1: Flow diagram of an SEIR model

5.3   The Basic Reproduction Number

Definition 5.3.1. The basic reproduction number $\mathscr{R}_0$ can be defined as the expected number of secondary infection cases produced directly by a single infectious individual assuming that the population is susceptible [43].

In other words, $\mathscr{R}_0$ is a measure of the potential of an infectious disease to spread in a population. If $\mathscr{R}_0 < 1$, then the number of infection cases will decay until the disease vanishes from the population. On the other hand, in case $\mathscr{R}_0 > 1$, then the disease is going to persist [43].

5.3.1   Basic Reproduction Number Calculation

For a compartmental ODE disease transmission model, $\mathscr{R}_0$ could be calculated by the following steps [42]:

1. Firstly, The system of ODE of disease compartments is represented in the following

form:

$$\dot{X} = \mathscr{F} - \mathscr{V}$$

Where $\mathscr{F} \in \mathbb{R}^n$ represents secondary infections, and $\mathscr{V} \in \mathbb{R}^n$ represents disease progression, recovery, or death.

2. Secondly, $\dot{X}$ is linearized about the disease free equilibrium point to get the following decoupled form:

$$\dot{X} = (F - V)X$$

Where the infection matrix F, and the transition matrix V are $n \times n$ matrices whose (i,j) entries are given by:

$$F = \frac{\partial \mathscr{F}_i}{\partial X_j} \quad , V = \frac{\partial \mathscr{V}_i}{\partial X_j}$$

3. Lastly, the next generation matrix $K = FV^{-1}$ is calculated, and $\mathscr{R}_0$ is simply the eigen value of K with the biggest modulus.

5.4 Sensitivity Index

In a model, to measure the relative change of a variable with respect to a parameter the sensitivity index of that variable with respect to the parameter is calculated. If the variable is differentiable with respect to the parameter, then the sensitivity index can be calculated using the following formula [44]:

$$\Upsilon_\theta^x = \frac{\partial x}{\partial \theta} \frac{\theta}{x}$$

Were x is the variable, and θ is the parameter.

Chapter 6: The Impact of COVID-19 on Patients with Comorbidity

6.1   Problem Statement

Individuals with diabetes have weakened immune functions. As a result, diabetic individuals were found to be at more risk of becoming critically ill when infected with a viral or bacterial infection as witnessed in the previous pandemics including SARS-CoV-1, H1N1, and MERS [45]. This was also found in the case of COVID-19 as suggested by many reports and studies. For instance, The Chinese Center for Disease Control and Prevention reported that the fatality rate of diabetic COVID-19 patients was 7.3% based on a report of 44,672 patients. Another study showed that 72% of COVID-19 patients with comorbidities including diabetes required admission to an ICU according to a study of 139 patients [45]. More generally, COVID-19 patients with not only diabetes, but other comorbidities such as cardiovascular diseases ,hypertension, lung diseases and kidney diseases were found to constitute the majority of higher morbidity and fatality cases [46, 47, 48].

As mentioned in Chapter 1, COVID-19 is a highly transmissible disease with many asymptomatic infection cases, making this disease very difficult to control and manage, and especially dangerous for the comorbidity population. Since the disease is highly contagious and is rapidly transmitting, it is crucial to find a way to control the spread of this disease. Mathematical modeling is a possible method to rapidly analyze the disease spread and develop a strategy to control it [49].

6.2 Thesis Contribution

The second part of this thesis presents a COVID-19 compartmental disease transmission model in the form of a system of ODEs. As previously stated, individuals with comorbidities are medically vulnerable, and so they are at a greater risk of developing critical disease complications in case they get infected, and they also have a higher fatality risk due to this contagious disease. Consequently, the presented model is focused on the populations of comorbidity. This model is an extended SEIR model that divides the population into: susceptible (S), exposed (E), mildly infected (I), asymptomatically infected (A), and treated populations (J) with and without comorbidity. It also includes the recovered (R), critically ill infected (C), and fatality populations (D).

The model can be used to represent the population of any city, country, or region. This can be done by estimating the parameters after fitting the model into the real data of the number of active infection cases in the desired population. In the presented case, the model is made to represent the population of the United Arab Emirates Country. The considered timeline is between the 22nd of January 2020 until the 27th of June 2020.

Calculations of the basic reproduction number are included. These calculations will help get an insight on how rapid the disease is being transmitted. Additionally, calculations of the sensitivity indices of the basic reproduction number with respect to the model's parameters are calculated. With the help of the sensitivity indices, the major factors that contributes to the disease transmission can be determined. Hence, by utilizing the calculations obtained, disease transmission control strategies can be developed.

6.3 Disease Transmission Model of COVID-19

The proposed mathematical model of the transmission of COVID-19 is given by the following system of ODEs:

$$
\begin{aligned}
\dot{S}_1 &= -(\beta_{I_1}^1 I_1 + \beta_{A_1}^1 A_1 + \beta_{I_2}^1 I_2 + \beta_{A_2}^1 A_2)S_1 \\
\dot{S}_2 &= -(\beta_{I_1}^2 I_1 + \beta_{A_1}^2 A_1 + \beta_{I_2}^2 I_2 + \beta_{A_2}^2 A_2)S_2 \\
\dot{E}_1 &= (\beta_{I_1}^1 I_1 + \beta_{A_1}^1 A_1 + \beta_{I_2}^1 I_2 + \beta_{A_2}^1 A_2)S_1 - (\gamma_1 + \nu_1)E_1 \\
\dot{E}_2 &= (\beta_{I_1}^2 I_1 + \beta_{A_1}^2 A_1 + \beta_{I_2}^2 I_2 + \beta_{A_2}^2 A_2)S_2 - (\gamma_2 + \nu_2)E_2 \\
\dot{A}_1 &= \gamma_1 E_1 - (\kappa_1 + \varphi_1 + \alpha_{A_1})A_1 \\
\dot{A}_2 &= \gamma_2 E_2 - (\kappa_2 + \varphi_2 + \alpha_{A_2})A_2 \\
\dot{I}_1 &= \kappa_1 A_1 + \nu_1 E_1 - (\xi_1 + \alpha_{I_1})I_1 \\
\dot{I}_2 &= \kappa_2 A_2 + \nu_2 E_2 - (\xi_2 + \alpha_{I_2})I_2 \\
\dot{J}_1 &= \varphi_1 A_1 + \xi_1 I_1 - \alpha_{J_1} J_1 \\
\dot{J}_2 &= \varphi_2 A_2 + \xi_2 I_2 - (\eta + \alpha_{J_2})J_2 \\
\dot{R} &= \alpha_{A_1}A_1 + \alpha_{A_2}A_2 + \alpha_{I_1}I_1 + \alpha_{I_2}I_2 + \alpha_{J_1}J_1 + \alpha_{J_2}J_2 + \alpha_C C \\
\dot{C} &= \eta J_2 - (\mu + \alpha_C)C \\
\dot{D} &= \mu C
\end{aligned}
\tag{6.1}
$$

Sub populations: In this compartmental ODE model, the populations S, E, A, I, and J are indexed by either 1 or 2. Index 1 represents a population without comorbidity, while index 2 represents a population with comorbidity. The recovered population R includes all individuals that have recovered with and without comorbidity. It is assumed that only individuals with comorbidity can develop a critical condition due to COVID-19. Therefore, the population C only includes individulas with comorbidities. Likewise,

it is also assumed that death due to COVID-19 only constitutes comorbidity population. Hence, population D is the fatality population of those who were infected with COVID-19 with a comorbidity. Since the considered timeline is somewhat short, the total population N is considered to be constant, i.e.

$$N = S_1 + S_2 + E_1 + E_2 + A_1 + A_2 + I_1 + I_2 + J_1 + J_2 + C + R + D = constant$$

Infection: In this model, it is assumed that new infection cases arise when a susceptible individual from S_1 or S_2 comes into contact with either a mildly infected individual from I_1 or I_2, or an asymptomatically infected individual from A_1 or A_2. It assumed that infected people who are being treated from J_1 or J_2 do not cause any secondary infections as they are isolated in a hospital. The same situation applies for infected individuals with a critical condition from C.

Parameters: parameters of the form β_y^x represents the disease transmission rate from an individual of population y to an individual from population x. The parameters γ and ν represents the rate at which an exposed individual progresses from the exposed class to the asymptomatic and the mildly infected classes respectively. The recovery rates are represented by the α parameters. An individual with comorbidity that is under treatment develops a critical condition at the rate η, and an individual under critical condition has a death rate of μ due to COVID-19 .

The model's disease progression is portrayed by the flow chart in Figure 6.1.
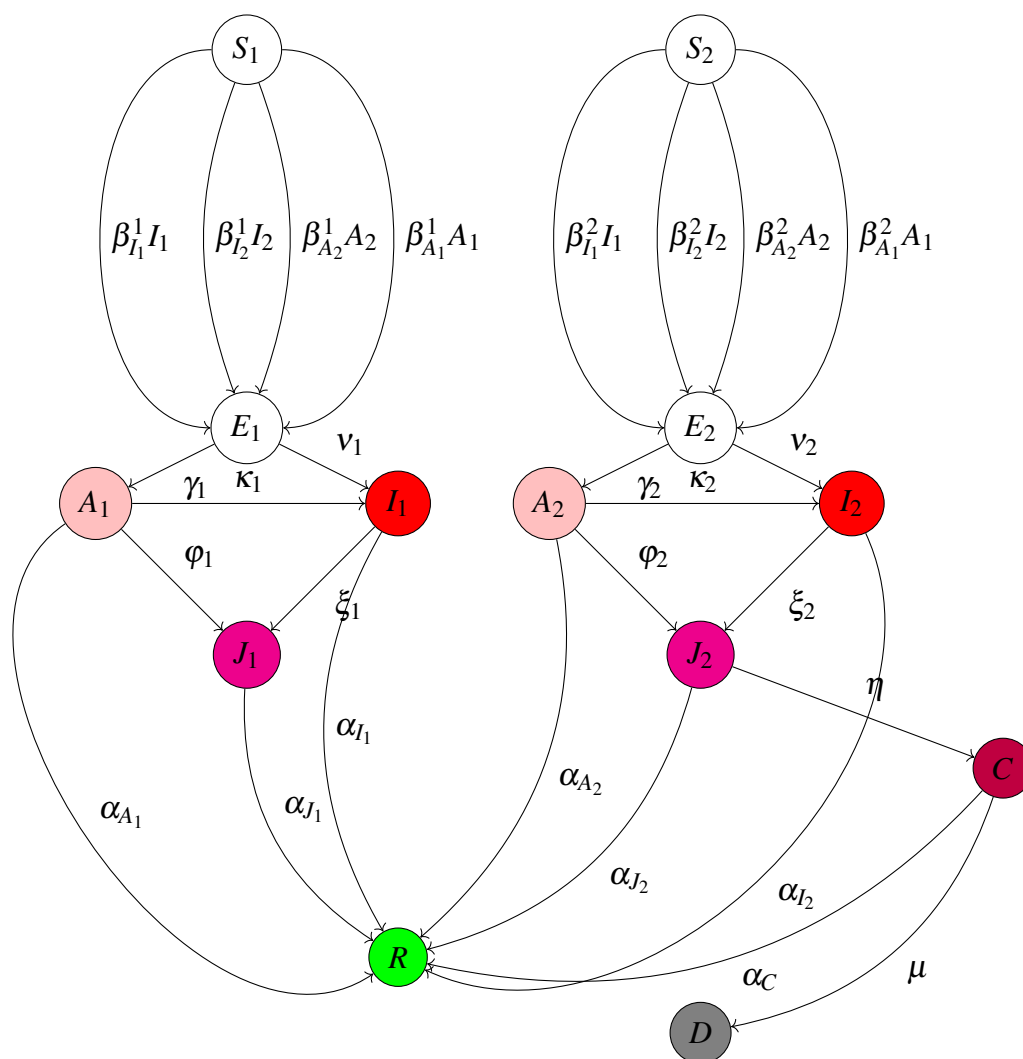
Figure 6.1: Flow chart of COVID-19 transmission model

6.4   Data Acquisition and Parameter Estimation

As a first step to estimate the model's parameters, some key parameters of the COVID-19

pandemic were estimated using data from china, the country with the first reported cases

of the disease. These estimations are presented in Table 6.1.

Table 6.1: Estimations of key parameters of COVID-19

Parameter	Symbol	Value (s)	Reference (s)
Fraction of asymptomatic infections	FracA	20 - 40%	[50, 51, 52, 53]
Duration of the infectious phase of the incubation period (days)	PresPer	2	
Duration of asymptomatic infections (days)	DurA	4 - 9.5	[54]
Average incubation period (days)	IncPer	4 - 9	[50, 55, 56, 57, 58] [59, 60]
Average duration of mild infections	DurMInf	4 - 20	[54, 60, 61, 46, 62]
Average fraction of mild symptomatic infections	FracMInf	27 - 81%	[54, 58, 63]
Average fraction of severe symptomatic infections	FracSev	14 - 24 %	[54, 58, 63]
Average fraction of critical symptomatic infections	FracCri	2 - 6%	[54, 58, 63, 64]
Average hospitalization duration (days)	DurHos	8 - 23	[46, 64, 65, 66, 67] [68, 69]
Average ICU admission duration (days)	TimeICU	21	
Probability of death due to the infection	ProbDeath	0.04 - 7.71%	WHO
Average time in the ICU until death (days)	TimeICUdeath	8 - 10	[62, 70]

Note: Since Model 6.1 is intended to represent the spread of COVID-19 in the United

Arab Emirates, the probability of death in Table 6.1 is based on the COVID-19 fatality

percentages of some of the Arab countries obtained from data provided by WHO during

the considered period.

For the second step, the model's parameters were given initial estimated values that are calculated based on the COVID-19 parameters presented in Table 6.1. These initial values are presented in Table 6.2.

Table 6.2: The estimated parameter values

Parameter	Symbol	Value for $i = 1$	Value for $i = 2$
Rate of progression from exposed to asymptomatic class	γ_i	0.5	0.5
Rate of progression from exposed mild symptoms class	ν_i	$\frac{1}{7}$	0.5
Rate at which the asymptomatic develops mild symptoms	κ_i	0.2025	$\frac{27}{950}$
Rate at which the asymptomatic becomes hospitalized	φ_i	0	0
Recovery rate of the asymptomatic populations	α_{A_i}	0.0475	$\frac{73}{950}$
Rate at which a mildly infected individual becomes hospitalized and isolated	ξ_i	0.007	0.06
Recovery rate of an infected individual with mild symptoms	α_{I_i}	0.043	0.1825
Rate at which a hospitalized individual develops a critical condition	η	-	$\frac{3}{1150}$
Recovery rate of hospitalized infected population	α_J	0.1225	$\frac{47}{1150}$
Recovery rate of an infected individual in the ICU	α_C	-	0.04395
Death rate of an individual in the ICU	μ	-	0.00964
Infection rate by a mildly infected individual	$\beta_{I_j}^i$	0.5944	1.68
Infection rate by an asymptomatically infected individual	$\beta_{A_j}^i$	0.5944	1.68

Note: the mathematical formulas used to calculate these parameters are presented in the Appendix in Table 6.

Thereafter, real data of the active infection cases in the United Arab Emirates were obtained from the 22nd of January 2020, to the 27th of June 2020. These numbers were obtained by subtracting the number of the recovery and death cases from the accumulated number of infection cases obtained from the World's Health Organization. Plots of the accumulated, recovered, death and active infection cases are presented in Figure 6.2 and Figure 6.3.
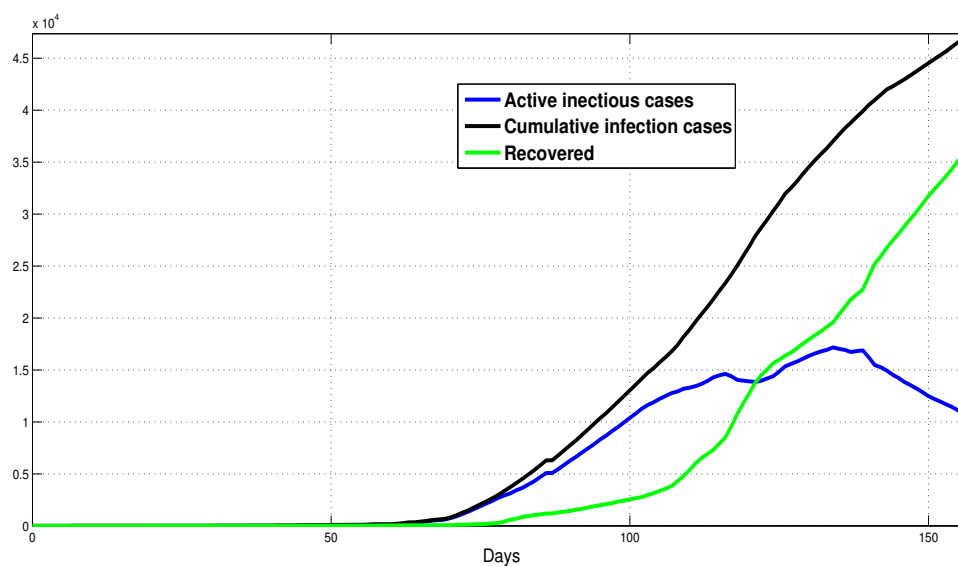
Figure 6.2: Active, recovered and accumulated infection cases in the UAE
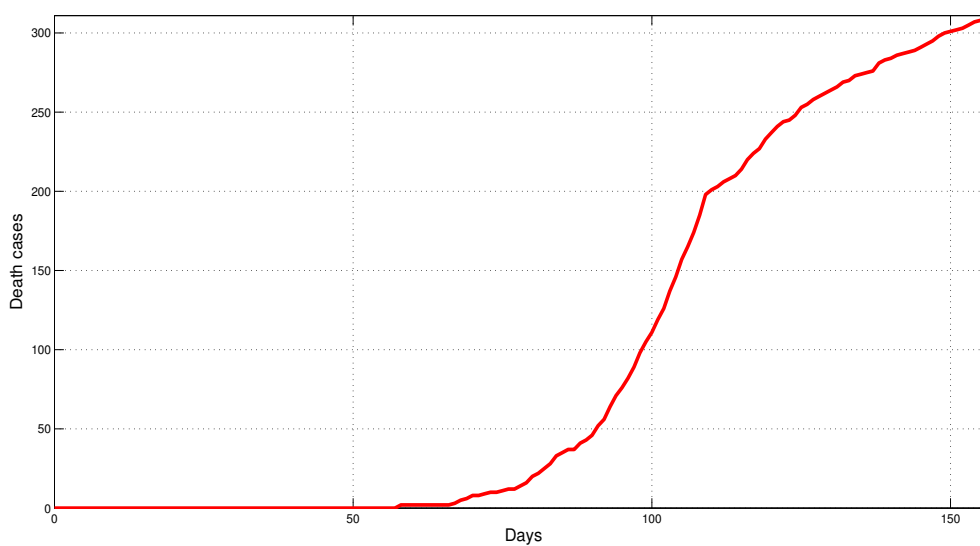
Figure 6.3: Death cases in the UAE

Next, using MATLAB, Model 6.1 was fitted to the real active infection cases as shown in Figure 6.4.
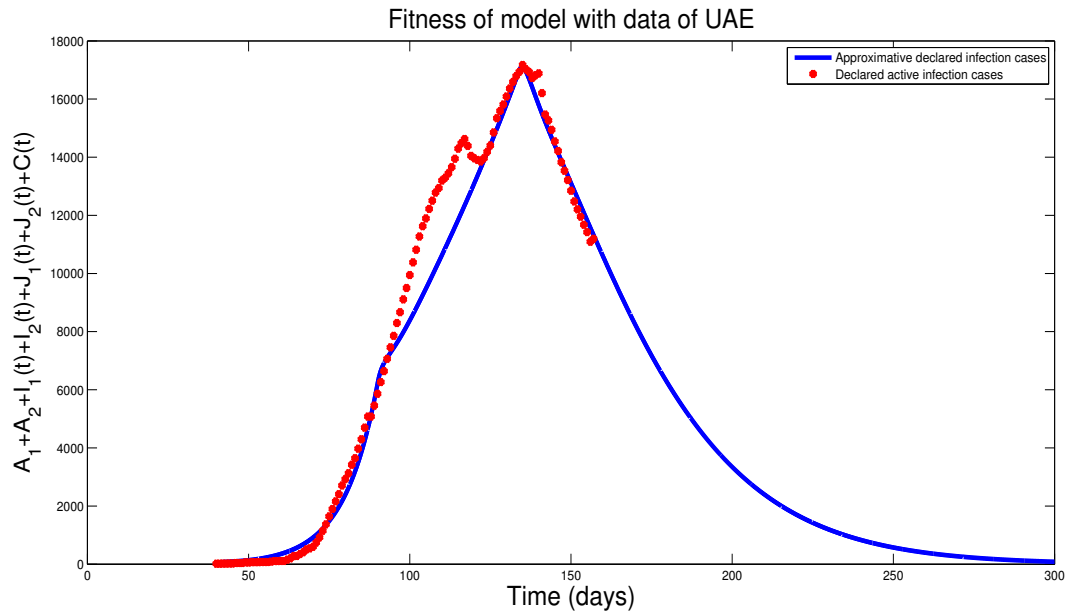
Figure 6.4: Fitting model's infection cases with real infection cases

The active infection cases of the model were considered to be:

$$\text{active infection cases} = A_1 + A_2 + I_1 + I_2 + J_1 + J_2 + C$$

Note: The exposed populations E_1, and E_2 were not considered as active infection cases as they include latently infected individuals whose infection is not active and they are not yet infectious.

The fitted parameters values are presented in Table 6.3.

Table 6.3: Fitted parameter values

Parameter	Value
γ_1	0.5
γ_2	0.5
ν_1	0.14286
ν_2	0.5
κ_1	0.2025
κ_2	0.02842
φ_1	0
φ_2	0
α_{A_1}	0.0475
α_{A_2}	0.07684
ξ_1	0.007
ξ_2	0.06
α_{I_1}	0.043
α_{I_2}	0.1825
η	0.0025
α_{J_1}	0.1225
α_{J_2}	0.04087
α_C	0.0476
μ	0.00004

Before analyzing the spread of COVID-19 in the United Arab Emirates, the basic reproduction number is calculated as it is needed for the analysis.

6.5 The Basic Reproduction Number

The infection compartments are represented by the disease state vector $\vec{X}$ which is expressed as:

$$\vec{X} = \begin{bmatrix} E_1 & E_2 & A_1 & A_2 & I_1 & I_2 \end{bmatrix}^T$$

$\dot{X}$ can be expressed in the following form:

$$\dot{X} = \frac{d\vec{X}}{dt} = \mathscr{F}(X) - \mathscr{V}(X)$$

Where,

$$\mathscr{F} = \begin{bmatrix} (\beta_{I_1}^1 I_1 + \beta_{A_1}^1 A_1 + \beta_{I_2}^1 I_2 + \beta_{A_2}^1 A_2)S_1 \\ (\beta_{I_1}^2 I_1 + \beta_{A_1}^2 A_1 + \beta_{I_2}^2 I_2 + \beta_{A_2}^2 A_2)S_2 \\ 0 \\ 0 \\ 0 \\ 0 \end{bmatrix} \qquad \mathscr{V} = \begin{bmatrix} (\gamma_1 + v_1)E_1 \\ (\gamma_2 + v_2)E_2 \\ -\gamma_1 E_1 + (\kappa_1 + \varphi_1 + \alpha_{A_1})A_1 \\ -\gamma_2 E_2 + (\kappa_2 + \varphi_2 + \alpha_{A_2})A_2 \\ -\kappa_1 A_1 - v_1 E_1 + (\xi_1 + \alpha_{I_1})I_1 \\ -\kappa_2 A_2 - v_2 E_2 + (\xi_2 + \alpha_{I_2})I_2 \end{bmatrix}$$

After linearizing the model about the disease-free equilibrium point, the following decoupled form is obtained:

$$\dot{X} = (F - V)X$$

Where the infection matrix F is given by:

$$F = \begin{bmatrix} 0 & 0 & \beta_{A_1}^1 S_1^o & \beta_{A_2}^1 S_1^o & \beta_{I_1}^1 S_1^o & \beta_{I_2}^1 S_1^o \\ 0 & 0 & \beta_{A_1}^2 S_2^o & \beta_{A_2}^2 S_2^o & \beta_{I_1}^2 S_2^o & \beta_{I_2}^2 S_2^o \\ 0 & 0 & 0 & 0 & 0 & 0 \\ 0 & 0 & 0 & 0 & 0 & 0 \\ 0 & 0 & 0 & 0 & 0 & 0 \\ 0 & 0 & 0 & 0 & 0 & 0 \end{bmatrix}$$

Here, S_1^o and S_2^o denotes the disease-free equilibrium populations with and without comorbidity.

The transition matrix V is given by, $V =$

$$
\begin{bmatrix}
(\gamma_1 + \nu_1) & 0 & 0 & 0 & 0 & 0 \\
0 & (\gamma_2 + \nu_2) & 0 & 0 & 0 & 0 \\
-\gamma_1 & 0 & (\kappa_1 + \varphi_1 + \alpha_{A_1}) & 0 & 0 & 0 \\
0 & -\gamma_2 & 0 & (\kappa_2 + \varphi_2 + \alpha_{A_2}) & 0 & 0 \\
-\nu_1 & 0 & -\kappa_1 & 0 & (\xi_1 + \alpha_{I_1}) & 0 \\
0 & -\nu_2 & 0 & -\kappa_2 & 0 & (\xi_2 + \alpha_{I_2})
\end{bmatrix}
$$

The inverse matrix of V is expressed as, $V^{-1} =$

$$
\begin{bmatrix}
\frac{1}{(\gamma_1+\nu_1)} & 0 & 0 & 0 & 0 & 0 \\
0 & \frac{1}{(\gamma_2+\nu_2)} & 0 & 0 & 0 & 0 \\
\frac{\gamma_1}{(\gamma_1+\nu_1)(\kappa_1+\varphi_1+\alpha_{A_1})} & 0 & \frac{1}{(\kappa_1+\varphi_1+\alpha_{A_1})} & 0 & 0 & 0 \\
0 & \frac{\gamma_2}{(\gamma_2+\nu_2)(\kappa_2+\varphi_2+\alpha_{A_2})} & 0 & \frac{1}{(\kappa_2+\varphi_2+\alpha_{A_2})} & 0 & 0 \\
\frac{\gamma_1\kappa_1+\nu_1(\kappa_1+\varphi_1+\alpha_{A_1})}{(\gamma_1+\nu_1)(\kappa_1+\varphi_1+\alpha_{A_1})(\xi_1+\alpha_{I_1})} & 0 & \frac{\kappa_1}{(\kappa_1+\varphi_1+\alpha_{A_1})(\xi_1+\alpha_{I_1})} & 0 & \frac{1}{(\xi_1+\alpha_{I_1})} & 0 \\
0 & \frac{\gamma_2\kappa_2+\nu_2(\kappa_2+\varphi_2+\alpha_{A_2})}{(\gamma_2+\nu_2)(\kappa_2+\varphi_2+\alpha_{A_2})(\xi_2+\alpha_{I_2})} & 0 & \frac{\kappa_2}{(\kappa_2+\varphi_2+\alpha_{A_2})(\xi_2+\alpha_{I_2})} & 0 & \frac{1}{(\xi_2+\alpha_{I_2})}
\end{bmatrix}
$$

Therefore, the next generation matrix K is expressed as, $K =$

$$
\begin{bmatrix}
(\phi_1\beta^1_{A_1} + \phi_2\beta^1_{I_1})S^o_1 & (\phi_3\beta^1_{A_2} + \phi_4\beta^1_{I_2})S^o_1 & (\phi_5\beta^1_{A_1} + \phi_6\beta^1_{I_1})S^o_1 & (\phi_7\beta^1_{A_2} + \phi_8\beta^1_{I_2})S^o_1 & \frac{\beta^1_{I_1}s^o_1}{(\xi_1+\alpha_{I_1})} & \frac{\beta^1_{I_2}s^o_1}{(\xi_2+\alpha_{I_2})} \\
(\phi_1\beta^2_{A_1} + \phi_2\beta^2_{I_1})S^o_2 & (\phi_3\beta^2_{A_2} + \phi_4\beta^2_{I_2})S^o_2 & (\phi_5\beta^2_{A_1} + \phi_6\beta^2_{I_1})S^o_2 & (\phi_7\beta^2_{A_2} + \phi_8\beta^2_{I_2})S^o_2 & \frac{\beta^2_{I_1}s^o_2}{(\xi_1+\alpha_{I_1})} & \frac{\beta^2_{I_2}s^o_2}{(\xi_2+\alpha_{I_2})} \\
0 & 0 & 0 & 0 & 0 & 0 \\
0 & 0 & 0 & 0 & 0 & 0 \\
0 & 0 & 0 & 0 & 0 & 0 \\
0 & 0 & 0 & 0 & 0 & 0
\end{bmatrix}
$$

Given the following:

$$\phi_1 = \frac{\gamma_1}{(\gamma_1+\nu_1)(\kappa_1+\varphi_1+\alpha_{A_1})} \quad \phi_2 = \frac{(\gamma_1\kappa_1+\nu_1(\kappa_1+\varphi_1+\alpha_{A_1}))}{(\gamma_1+\nu_1)(\kappa_1+\varphi_1+\alpha_{A_1})(\xi_1+\alpha_{I_1})}$$

$$\phi_3 = \frac{\gamma_2}{(\gamma_2+\nu_2)(\kappa_2+\varphi_2+\alpha_{A_2})} \quad \phi_4 = \frac{(\gamma_2\kappa_2+\nu_2(\kappa_2+\varphi_2+\alpha_{A_2}))}{(\gamma_2+\nu_2)(\kappa_2+\varphi_2+\alpha_{A_2})(\xi_2+\alpha_{I_2})}$$

$$\phi_5 = \frac{1}{(\kappa_1+\varphi_1+\alpha_{A_1})} \quad \phi_6 = \frac{\kappa_1}{(\kappa_1+\varphi_1+\alpha_{A_1})(\xi_1+\alpha_{I_1})} = \phi_5\frac{\kappa_1}{(\xi_1+\alpha_{I_1})}$$

$$\phi_7 = \frac{1}{(\kappa_2+\varphi_2+\alpha_{A_2})} \quad \phi_8 = \frac{\kappa_2}{(\kappa_2+\varphi_2+\alpha_{A_2})(\xi_2+\alpha_{I_2})} = \phi_7\frac{\kappa_2}{(\xi_1+\alpha_{I_2})}$$

Then, $\mathscr{R}_0$ is the eigenvalue of matrix K with the biggest modulus which is given by:

$$\mathscr{R}_0 = \frac{1}{2}\left(\sqrt{(\mathscr{R}_{01}-\mathscr{R}_{02})^2+4\bar{\mathscr{R}}_{01}\bar{\mathscr{R}}_{02}}+\mathscr{R}_{01}+\mathscr{R}_{02}\right)$$

Where

$$\mathscr{R}_{01} = (\phi_1\beta_{A_1}^1+\phi_2\beta_{I_1}^1)S_1^o, \quad \bar{\mathscr{R}}_{01} = (\phi_3\beta_{A_2}^1+\phi_4\beta_{I_2}^1)S_1^o$$

$$\mathscr{R}_{02} = (\phi_3\beta_{A_2}^2+\phi_4\beta_{I_2}^2)S_2^o, \quad \bar{\mathscr{R}}_{02} = (\phi_1\beta_{A_1}^2+\phi_2\beta_{I_1}^2)S_2^o$$

This indicates that $\mathscr{R}_0$ depends on four components which can be viewed as sub basic reproduction numbers. $\mathscr{R}_{01}$ represents the basic reproduction number of the non-comorbidity population on its own, $\mathscr{R}_{02}$ represents the basic reproduction number of the comorbidity population, $\bar{\mathscr{R}}_{01}$ represents the basic reproduction number of the infection of the non-comorbidity population that is caused by the comorbidity population and $\bar{\mathscr{R}}_{02}$ represents the basic reproduction number of the comorbidity population infections which are caused by the non-comorbidity population. Hence, different population distributions results in different reproduction numbers as indicated by the following scenarios:

Case 1: $\bar{\mathscr{R}}_{01} = 0$

In this case no infection of the general population is caused by the comorbidity population. This is achieved by isolating individuals with comorbidity from the

general population. The basic reproduction number in this case is:

$$\mathcal{R}_0 = \frac{1}{2}(\sqrt{(\mathcal{R}_{01} - \mathcal{R}_{02})^2} + \mathcal{R}_{01} + \mathcal{R}_{02}) = \mathcal{R}_{01}$$

indicating that infection will only be spread among the non-comorbidity population and the disease will not be transmitted from or to the comorbidity population. In this scenario the following points can be drawn:

$\mathcal{R}_0 > 1$:   when $\mathcal{R}_{01} > 1$

$\mathcal{R}_0 < 1$:   when $\mathcal{R}_{01} < 1$

Indicating that disease transmission depends completely on the general population.

Case 2: $\bar{\bar{\mathcal{R}}}_{02} = 0$

In this case no disease transmission from the general population to the comorbidity population takes place. This case has the same result as case 1.

Note: The previous two cases are examples of shielding which is a method utilized by the governments of many countries to prevent disease spread amongst people who are medically vulnerable. These people includes elderly, people suffering from heart or respiratory diseases in addition to pregnant women. In this method, these people isolate themselves and practice social distancing as much as possible in order to protect themselves.

Case 3: $\mathcal{R}_{01}, \mathcal{R}_{02}, \bar{\bar{\mathcal{R}}}_{01}$ and $\bar{\bar{\mathcal{R}}}_{01}$ are constants. In this case the disease is being transmitted in a constant, stable way amongst the different populations. In this case $\mathcal{R}_0 < 1$ holds when:

$$\frac{1}{2}(\sqrt{(\mathcal{R}_{01} - \mathcal{R}_{02})^2 + 4\bar{\bar{\mathcal{R}}}_{01}\bar{\bar{\mathcal{R}}}_{02}} + \mathcal{R}_{01} + \mathcal{R}_{02}) < 1$$

which implies that

$$\sqrt{(\mathscr{R}_{01} - \mathscr{R}_{02})^2 + 4\bar{\mathscr{R}}_{01}\bar{\mathscr{R}}_{02}} < 2 - \mathscr{R}_{01} - \mathscr{R}_{02}$$

in case

$$|\mathscr{R}_{01} - \mathscr{R}_{02}| < 2 - \mathscr{R}_{01} - \mathscr{R}_{02}$$

which applies when $\max\{\mathscr{R}_{01}, \mathscr{R}_{02}\} < 1$, implying that the disease will stop spreading once it stops spreading amongst both the general and the comorbidity populations. Similarly, $\mathscr{R}_0 > 1$ when:

$$\frac{1}{2}(\sqrt{(\mathscr{R}_{01} - \mathscr{R}_{02})^2 + 4\bar{\mathscr{R}}_{01}\bar{\mathscr{R}}_{02}} + \mathscr{R}_{01} + \mathscr{R}_{02}) > 1,$$

which implies that

$$\sqrt{(\mathscr{R}_{01} - \mathscr{R}_{02})^2 + 4\bar{\mathscr{R}}_{01}\bar{\mathscr{R}}_{02}} > 2 - \mathscr{R}_{01} - \mathscr{R}_{02}$$

which applies when $\min\{\mathscr{R}_{01}, \mathscr{R}_{02}\} > 1$ indicating that the disease will continue to spread as long as it is still spreading amongst both the general and the comorbidity populations.

6.6 Analyzing the Spread of COVID-19 in the UAE

In this section, the spread of COVID-19 in the United Arab Emirates is analyzed using Model (6.1). The considered timeline is from the 22nd of January 2020, to the 27th of June 2020. In the model, the 22nd of January is denoted by $t = 0$, and the 27th of June 2020 is denoted by $t = 157$, where t represents the days.

Stages of measures: The considered timeline can be divided into three stages based on the measures the authorities of the United Arab Emirates took to help in reducing the spread of COVID-19. These stages are given by:

Stage 1 (No intervention): This stage was at the beginning of the pandemic. Hence, the number of cases was not significant. The country's authorities observed the evolution of the infection cases in this stage and started to prepared a proper strategy for reducing the spread of COVID-19. At this stage, the transmission rate can be considered to be constant.

Stage 2 (Slightly effective intervention): At this stage, the number of cases has significantly increased. Hence, the concerned authorities used a series of measures to help reducing the spread of COVID-19. These measures included switching to remote working for applicable jobs, in addition to virtual learning for students. Moreover, many malls and shops were temporarily closed and a nationwide disinfection program was established [71]. These measures helped in relenting the spread of COVID-19 but were not very effective, as the number of active infection cases continued to rise. At this stage, the transmission rate was reduced, but can also be considered to be constant.

Stage 3 (Effective intervention): At this stage, authorities imposed a full lock-down on the country. This measure led to a significant decrease in the mobility of people in the UAE as indicated by Apple's and Google's mobility reports [72, 73]. Naturally, the transmission rate has decreased at this stage, and the number of active infection cases have started to decrease as well.

Figure 6.5 shows the three mentioned stages represented by an active infection case timeline.
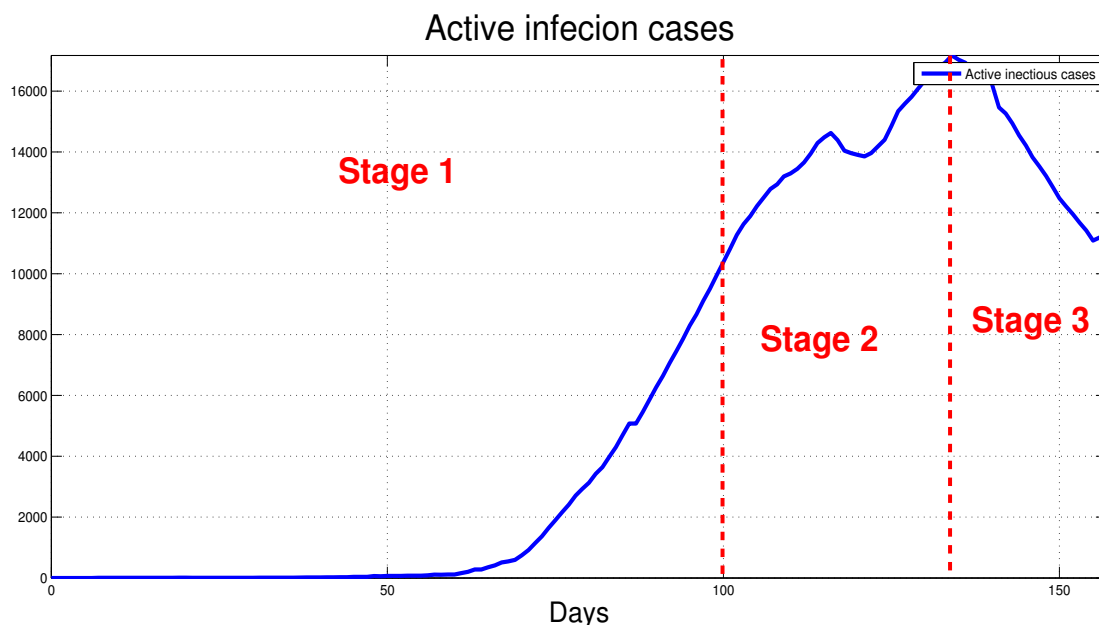
Figure 6.5: The three stages of measures taken by the UAE authorities

Approximating disease-free equilibrium populations: At the disease-free equilibrium, the population with comorbidity S_2^o is approximated by the population aged 55 years old and above. This approximation is based on a study on the severity of COVID-19. In this study, data were collected from the different regions of china including Wuhan where the virus is originated. The study showed that the fatality rate is higher amongst the populations aged 50 and above [69].

In the UAE, the population aged $55 - 64$ makes up 7.68% of the total population, and the population aged 65 years and above makes up 1.9% of the total population, meaning that the population with comorbidity is approximated by 9.58% of the total population of $9,992,083$ as in july 2020 [74]. Hence, $S_2^o \approx 957242$ and $S_1^o \approx 9034841$. The comorbidity percentage is denoted by $p = 9.58\%$.

Using a similar method, the number of people with comorbidity in the different

subpopulations can be approximated. For simplicity, it is presumed that $\beta_{I_1}^1 = \beta_{I_1}^2$, $\beta_{I_2}^1 = \beta_{I_2}^2$, $\beta_{A_1}^1 = \beta_{A_1}^2$ and $\beta_{A_2}^1 = \beta_{A_2}^2$, which means that an individual in the same class of infection has the same transmission rate (mobility).

The transmission rate of the asymptomatic individuals depends on their mobility, where infected individuals of this category do not show any symptoms, and therefore infect others without being revealed. Individuals of this category constitutes most of the careless individuals who does not respect the restrictions imposed by the government. Using the mobility reports [72, 73] it can deduced that there is a decrease of $55 - 60\%$ in the mobility at parks. Implying that $40 - 45\%$ of the population did not respect the measures taken by the government. Hence, the mobility rate is denoted by $p_1 = 40\%$. And so, it can be assumed that $\beta_{A_i}^j = p_1 \beta_{I_i}^j$ for $i, j = 1, 2$. Now it remains to determine the transmission rates $\beta_{I_i}^1$, $i = 1, 2$.

The transmission rates β are assumed to have the following form:

$$
\beta_{I_i}^1 = \begin{cases} \beta_i, & t \in [0, 100] & \text{(Stage 1)} \\ 38.5\% \beta_i, & t \in [100, 140] & \text{(Stage 2)} \\ 38.5\% \beta_i \exp^{-\delta t}, & t \in [145, 157] & \text{(Stage 3)} \end{cases} \quad (6.2)
$$

where $\delta = 0.0265$ denotes the lock-down efficiency rate. Using these approximations, it is deduced that: $\beta_1 = 2.1 \times 10^{-8}$ and $\beta_2 = 4 \times 10^{-9}$.

Using the approximated parameter values of Model 6.1 in Table 6.3, and the approximated transmission rates, the number of individuals in each infection class can be approximated as shown in the following timeline.
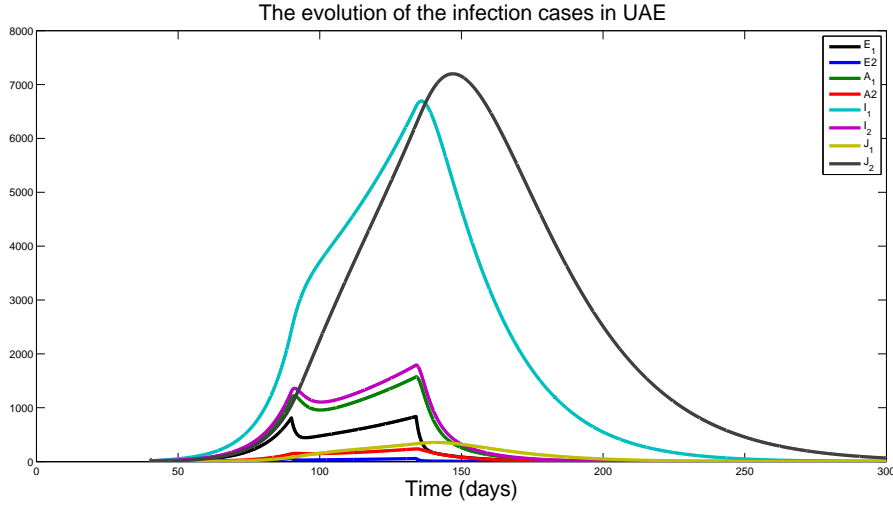
Figure 6.6: Infection cases in each class

By taking a closer look at Figure 6.6, one can note that the number of the mildly infected individuals without comorbidity (I_1) is far greater than the one with co-morbidity (I_2). The same remark can be noted for the A and E classes. This is a very important remark as it indicates that the UAE community have implemented a shielding behavior that isolates the comorbidity population in order to protect them.

Now, using the previously mentioned approximations the following values are obtained:

$$\phi_1 = 3.1111, \quad \phi_5 = 4$$

$$\phi_2 = 17.0444, \quad \phi_6 = 16.2$$

$$\phi_3 = 4.75, \quad \phi_7 = 9.5$$

$$\phi_4 = 2.6186, \quad \phi_8 = 1.1134$$

Therefore, the values of $\mathscr{R}_0$ corresponding to the three stages are given by:

Table 6.4: $\mathscr{R}_0$ on the different stages

Stage 1	Stage 2	Stage 3
$\mathscr{R}_0 = 3.4873$	$\mathscr{R}_0 = 1.3426$	$\mathscr{R}_0 = 0.0288 - 0.0209$

6.7 Sensitivity Analysis

Sensitivity analysis helps in determining how important each parameter is to disease transmission. Such an analysis is commonly used to determine how robust a model is to the predicted parameter values, since data collection and presumptions are usually accompanied with errors. Using the sensitivity index, parameters that have a high impact on $\mathscr{R}_0$ can be determined, and by using this knowledge an appropriate intervention strategy to help in reducing disease transmission can be implemented [44].

The sensitivity index of $\mathscr{R}_0$, which is differentiable with respect to a given parameter θ, is given by:

$$\Upsilon_\theta^{\mathscr{R}_0} = \frac{\partial \mathscr{R}_0}{\partial \theta} \frac{\theta}{\mathscr{R}_0}$$

The sensitivity index expressions of $\mathscr{R}_0$ with respect to the parameters of Model 6.1 are presented in the Appendix, and the values of these indices are presented in Table 6.5.

Looking at the sensitivity indices in Table 6.5, it can be noticed that all disease transmission parameters $\beta_{A_1}^1$, $\beta_{A_2}^1$, $\beta_{I_1}^1$, $\beta_{I_2}^1$, $\beta_{A_1}^2$, $\beta_{A_2}^2$, $\beta_{I_1}^2$ and $\beta_{I_2}^2$ have positive sensitivity indices, which indicates that clearly when disease transmission is increased, naturally the *basic reproduction number* will increase accordingly. Similarly, the recovery rates α_{I_1}, α_{I_2}, α_{A_1} and α_{A_2} have negative sensitivity indices, indicating that when the recovery rates increase, the *basic reproduction number* will decrease in response.

Table 6.5: The sensitivity indices of $\mathscr{R}_0$ with respect to the parameters

Parameter	Sensitivity Index
$\beta_{I_1}^1$	0.8890
κ_1	0.0740
$\beta_{A_1}^1$	0.0649
ν_1	0.0203
$\beta_{A_2}^1$	0.0200
γ_2	0.0094
$\beta_{I_1}^2$	0.0039
$\beta_{I_2}^1$	0.0028
$\beta_{A_1}^2$	0.0015
$\beta_{A_2}^2$	$4.7710 * 10^{-4}$
$\beta_{I_2}^2$	$6.5754 * 10^{-5}$
φ_1	0
φ_2	0
ξ_2	$-6.9826 * 10^{-4}$
α_{I_2}	-0.0021
κ_2	-0.0051
ν_2	-0.0094
α_{A_2}	-0.0154
γ_1	-0.0203
ξ_1	-0.1274
α_{A_1}	-0.1379
α_{I_1}	-0.7828

Note: The sensitivity indices of the parameters α_{J_1}, α_{J_2}, η and μ are zero since $\mathscr{R}_0$ does not depend on them as they don't involve disease transmission.
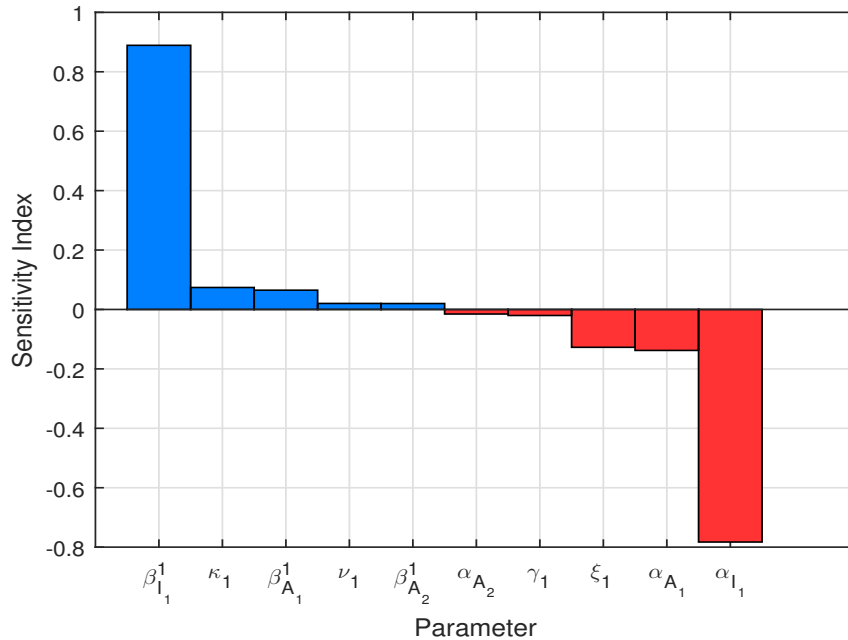
Figure 6.7: Sensitivity index bar chart

Figure 6.7 shows the sensitivity indices that has the most effect on $\mathscr{R}_0$. The values of the sensitivity indices indicates that $\beta_{I_1}^1$, and α_{I_1} are the parameters that effects the value of $\mathscr{R}_0$ the most, where $\beta_{I_1}^1$ has an index of $+0.8890$, and α_{I_1} has an index of -0.7828. Indicating that when $\beta_{I_1}^1$ increases by 100%, $\mathscr{R}_0$ increases by 88.9% as a response. Similarly, when α_{I_1} increases by 100%, $\mathscr{R}_0$ decreases by 78.28% accordingly.

6.8 Results and Discussions

Using Model 6.1 with its parameters, the following conclusions can be drawn :

1. The speed of the transmission of COVID-19 is determined by $\mathscr{R}_0$. More-over, since the stages with authority intervention had a smaller number of $\mathscr{R}_0$, then this indicates that clearly imposing lock-down / quarantine measures helps

greatly with reducing the transmission rate of COVID-19.

2. The parameters / factors with the major effects on $\mathscr{R}_0$ were the disease transmission and the recovery rates. This indicates that practicing social distancing to minimize contact between people, and enhancing the immune system to increase the recovery rate are the best solutions to reduce the speed of the disease spread and consequently diminish it.

However, the social distancing solution has its flaws. Firstly, it has a negative impact on the economy. This results from the fact that remote working is not as productive as working at the workplace. Additionally, many restaurants, hotels and gyms were bankrupt as they received little to no customers. Secondly, as for education, many students experienced difficulties with virtual learning as they cannot learn as efficiently, resulting in bad academic performance.

References

[1] American Diabetes Association. Diagnosis and classification of diabetes mellitus. *Diabetes care*, 37(Supplement 1):S62–S67, 2014. DOI: 10.2337/dc14-S081.

[2] International Diabetes Federation. IDF Diabetes Atlas. 9th ed. pages 10–70, 2019.

[3] M. Clark. *Understanding Diabetes*. John Wiley & Sons, 1 edition, 2004. DOI: 10.1002/0470030240.

[4] A. Makroglou, J. Li, and Y. Kuang. Mathematical models and software tools for the glucose-insulin regulatory system and diabetes: an overview. *Applied numerical mathematics*, 56(3-4):559–573, 2006.

[5] B. Abuyassin and I. Laher. Diabetes epidemic sweeping the Arab world. *World journal of diabetes*, 7(8):165–174, 2016.

[6] M. Alarouj, A. Bennakhi, Y. Alnesef, M. Sharifi, and N. Elkum. Diabetes and associated cardiovascular risk factors in the state of kuwait: the first national survey. *International Journal of Clinical Practice*, 67(1):89–96, 2013.

[7] R.A. Bacchus, J.L. Bell, M. Madkour, and B. Kilshaw. The prevalence of diabetes mellitus in male saudi arabs. *Diabetologia*, 23(4):330–332, 1982.

[8] A. Bener, M. Zirie, I.M. Janahi, A. Al-Hamaq, M. Musallam, and N.J. Wareham. Prevalence of diagnosed and undiagnosed diabetes mellitus and its risk factors in a population-based study of Qatar. *Diabetes research and clinical practice*, 84(1):99–106, 2009.

[9] World Health Organization et al. *Global status report on noncommunicable diseases 2014*. World Health Organization, 2014.

[10] A. Afshin, R. Micha, S. Khatibzadeh, S. Fahimi, P. Shi, J. Powles, G. Singh, M. Yakoob, M. Abdollahi, S. Al-Hooti, et al. The impact of dietary habits and metabolic risk factors on cardiovascular and diabetes mortality in countries of the Middle East and North Africa in 2010: a comparative risk assessment analysis. *BMJ open*, 5(5), 2015. DOI: 10.1136/bmjopen-2014-006385.

[11] E. Sharara, C. Akik, H. Ghattas, and C.M. Obermeyer. Physical inactivity, gender and culture in Arab countries: a systematic assessment of the literature. *BMC public health*, 18(1), 2018. DOI: 10.1186/s12889-018-5472-z.

[12] H. Saadi, S.G. Carruthers, N. Nagelkerke, F. Al-Maskari, B. Afandi, R. Reed, M. Lukic, M.G. Nicholls, E. Kazam, K. Algawi, et al. Prevalence of diabetes mellitus and its complications in a population-based sample in Al Ain, United Arab Emirates. *Diabetes research and clinical practice*, 78(3):369–377, 2007.

[13] International Diabetes Federation. IDF Diabetes Atlas. 8th ed. pages 72–73, 2017.

[14] C. Bommer, E. Heesemann, V. Sagalova, J. Manne-Goehler, R. Atun, T. Bärnighausen, and S. Vollmer. The global economic burden of diabetes in adults aged 20–79 years: a cost-of-illness study. *The lancet Diabetes & endocrinology*, 5(6):423–430, 2017.

[15] T. Singhal. A Review of Coronavirus Disease-2019 (COVID-19). *The Indian Journal of Pediatrics*, pages 281–286, 2020.

[16] L. Fang, G. Karakiulakis, and M. Roth. Are patients with hypertension and diabetes mellitus at increased risk for COVID-19 infection? *The Lancet Respiratory Medicine*, 2020. DOI: 10.1016/S2213-2600(20)30116-8.

[17] Z.T. Bloomgarden. Diabetes and COVID-19. *Journal of Diabetes*, 12(4):347–348, 2020.

[18] R.N. Bergman. Minimal model: perspective from 2005. *Hormone Research*, 64(Suppl. 3):8–15, 2005.

[19] M.K. Shukla, B.B. Sharma, and A.T. Azar. Control and synchronization of a fractional order hyperchaotic system via backstepping and active backstepping approach. In *Mathematical Techniques of Fractional Order Systems*, pages 559–595. Elsevier, 2018.

[20] Z. Fu, E.R. Gilbert, and D. Liu. Regulation of insulin synthesis and secretion and pancreatic beta-cell dysfunction in diabetes. *Current diabetes reviews*, 9(1):25–53, 2013.

[21] R.N. Bergman, L.S. Phillips, and C. Cobelli. Physiologic evaluation of factors controlling glucose tolerance in man: measurement of insulin sensitivity and beta-cell glucose sensitivity from the response to intravenous glucose. *The Journal of clinical investigation*, 68(6):1456–1467, 1981.

[22] E.L. Lozner, A.W. Winkler, F.H.L. Taylor, and J.P. Peters. The Intravenous Glucose Tolerance Test. *The Journal of clinical investigation*, 20(5):507–515, 1941.

[23] A.G. Gallardo-Hernández, M.A. González-Olvera, C. Revilla-Monsalve, J.A. Escobar, M. Castellanos-Fuentes, and R. Leder. Rapid automatic identification of parameters of the Bergman Minimal Model in Sprague-Dawley rats with experimental diabetes for adaptive insulin delivery. *Computers in biology and medicine*, 108:242–248, 2019.

[24] C. Cobelli, G. Federspil, G. Pacini, A. Salvan, and C. Scandellari. An Integrated Mathematical Model of the Dynamics of Blood Glucose and its Hormonal Control. *Mathematical Biosciences*, 58(1):27–60, 1982.

[25] M. Page. *BMA illustrated medical dictionary*. Dorling Kindersley Publishers Ltd, 2002.

[26] S. Rathee. ODE models for the management of diabetes: A review. *International Journal of Diabetes in Developing Countries*, 37(1):4–15, 2017.

[27] P. Palumbo, S. Ditlevsen, A. Bertuzzi, and A. De Gaetano. Mathematical modeling of the glucose–insulin system: A review. *Mathematical biosciences*, 244(2):69–81, 2013.

[28] A. D. Gaetano and O. Arino. Mathematical modelling of the intravenous glucose tolerance test. *Journal of mathematical biology*, 40(2):136–168, 2000.

[29] E. B. Lee and L. Markus. *Foundations of Optimal Control Theory*. John Wiley, 1967.

[30] L.C. Evans. An Introduction to Mathematical Optimal Control Theory. *Lecture Notes, University of California, Department of Mathematics, Berkeley*, 3:15–40, 2005.

[31] J. Löber. *Optimal Trajectory Tracking of Nonlinear Dynamical Systems*. Springer International Publishing, 2017. DOI: 10.1007/978-3-319-46574-6.

[32] H. Leiva. Rothe's fixed point theorem and controllability of semilinear nonautonomous systems. *Systems & Control Letters*, 67:14–18, 2014.

[33] H. Leiva, D. Cabada, and R. Gallo. Controllability of time-varying systems with impulses, delays and nonlocal conditions. *Afrika Matematika*, 2021. DOI: 10.1007/s13370-021-00872-y.

[34] C. Cobelli, E. Renard, and B. Kovatchev. Artificial Pancreas: Past, Present, Future. *Diabetes*, 60(11):2672–2682, 2011.

[35] W. Liu. A mathematical model for the robust blood glucose tracking. *Mathematical biosciences and engineering: MBE*, 16(2):759–781, 2019.

[36] J. Sturis, Eve E.V. Cauter, J.D. Blackman, and K.S. Polonsky. Entrainment of pulsatile insulin secretion by oscillatory glucose infusion. *The Journal of clinical investigation*, 87(2):439–445, 1991.

[37] D. Chalishajar, H. Chalishajar, and J. David. Trajectory Controllability of Nonlinear Integro-Differential System — An Analytical and a Numerical Estimations. *Applied Mathematics*, 3(11):1729–1738, 2012.

[38] L. Hogben. *Handbook of linear algebra*. CRC press, 2013. DOI: 10.1201/b16113.

[39] R. Meise and D. Vogt. *Introduction to Functional Analysis*. Clarendon Press, 1997.

[40] J. Zabczyk. *Mathematical Control Theory*. Springer, 2020. DOI: 10.1007/978-3-030-44778-6.

[41] Z. Ma, Y. Zhou, and J. Wu. *Modeling and Dynamics of Infectious Diseases*, volume 11. World Scientific Publishing Company, 2009. DOI: 10.1142/7223.

[42] P. Van den Driessche and J. Watmough. Further Notes on the Basic Reproduction Number. In *Mathematical epidemiology*, pages 159–178. Springer, 2008.

[43] M. Martcheva. *An Introduction to Mathematical Epidemiology*, volume 61. Springer, 2015. DOI: 10.1007/978-1-4899-7612-3.

[44] H. Rodrigues, M. Monteiro, and D. Torres. Sensitivity Analysis in a Dengue Epidemiological Model. *arXiv e-prints*, 2013. DOI: 10.1155/2013/721406.

[45] A.K. Singh, R. Gupta, A. Ghosh, and A. Misra. Diabetes in COVID-19: Prevalence, pathophysiology, prognosis and practical considerations. *Diabetes & Metabolic Syndrome: Clinical Research & Reviews*, 14(4):303–310, 2020.

[46] F. Zhou, T. Yu, R. Du, G. Fan, Y. Liu, Z. Liu, J. Xiang, Y. Wang, B. Song, X. Gu, et al. Clinical course and risk factors for mortality of adult inpatients with COVID-19 in Wuhan, China: a retrospective cohort study. *The lancet*, 395(10229):1054–1062, 2020.

[47] C. Sardu, J. Gambardella, M.B. Morelli, X. Wang, R. Marfella, and G. Santulli. Hypertension, Thrombosis, Kidney Failure, and Diabetes: is COVID-19 an Endothelial Disease? a Comprehensive Evaluation of Clinical and Basic Evidence. *Journal of clinical medicine*, 9(5):1417–1439, 2020. DOI: 10.3390/jcm9051417.

[48] S. Garg, L. Kim, M. Whitaker, A. O'Halloran, C. Cummings, R. Holstein, M. Prill, S. Chai, P. Kirley, N. Alden, et al. Hospitalization Rates and Characteristics of Patients Hospitalized with Laboratory-Confirmed Coronavirus Disease 2019—COVID-NET, 14 States, March 1–30, 2020. *Morbidity and mortality weekly report*, 69(15):458–464, 2020.

[49] C. I. Siettos and L. Russo. Mathematical modeling of infectious disease dynamics. *Virulence*, 4(4):295–306, 2013.

[50] Q. Bi, Y. Wu, S. Mei, C. Ye, X. Zou, Z. Zhang, X. Liu, L. Wei, S. Truelove, T. Zhang, et al. Epidemiology and Transmission of COVID-19 in Shenzhen China: Analysis of 391 cases and 1,286 of their close contacts. *MedRxiv*, 2020. DOI: 10.1101/2020.03.03.20028423.

[51] H. Nishiura, T. Kobayashi, T. Miyama, A. Suzuki, S. Jung, K. Hayashi, R. Kinoshita, Y. Yang, B. Yuan, Andrei R A. Akhmetzhanov, et al. Estimation of the asymptomatic ratio of novel coronavirus infections (COVID-19). *International journal of infectious diseases*, 94:154–155, 2020.

[52] K. Mizumoto, K. Kagaya, A. Zarebski, and G. Chowell. Estimating the Asymptomatic Ratio of 2019 Novel Coronavirus Onboard the Princess Cruises Ship, 2020. *MedRxiv*, 2020. DOI: 10.1101/2020.02.20.20025866.

[53] J. Liao, S. Fan, J. Chen, J. Wu, S. Xu, Y. Guo, C. Li, X. Zhang, C. Wu, H. Mou, et al. Epidemiological and Clinical Characteristics of COVID-19 in Adolescents and Young Adults. *The Innovation*, 1(1), 2020. DOI: 10.1016/j.xinn.2020.04.001.

[54] P. Yang, Y. Ding, Z. Xu, R. Pu, P. Li, J. Yan, J. Liu, F. Meng, L. Huang, L. Shi, et al. Epidemiological and clinical features of COVID-19 patients with and without pneumonia in Beijing, China. *Medrxiv*, 2020. DOI: 10.1101/2020.02.28.20028068.

[55] N.M. Linton, T. Kobayashi, Y. Yang, K. Hayashi, A.R. Akhmetzhanov, S. Jung, B. Yuan, R. Kinoshita, and H. Nishiura. Incubation Period and Other Epidemiological Characteristics of 2019 Novel Coronavirus Infections with Right Truncation: A Statistical Analysis of Publicly Available Case Data. *Journal of clinical medicine*, 9(2):538–547, 2020. DOI: 10.3390/jcm9020538.

[56] J.A. Backer, D. Klinkenberg, and J. Wallinga. Incubation period of 2019 novel coronavirus (2019-nCoV) infections among travellers from Wuhan, China, 20–28 January 2020. *Euro surveillance*, 25(5), 2020. DOI: 10.2807/1560-7917.ES.2020.25.5.2000062.

[57] S.A. Lauer, K.H. Grantz, Q. Bi, F.K. Jones, Q. Zheng, H.R. Meredith, A.S. Azman, N.G. Reich, and J. Lessler. The incubation period of coronavirus disease 2019 (COVID-19) from publicly reported confirmed cases: estimation and application. *Annals of internal medicine*, 172(9):577–582, 2020.

[58] A. Pan, L. Liu, C. Wang, H. Guo, X. Hao, Q. Wang, J. Huang, N. He, H. Yu, X. Lin, et al. Association of public health interventions with the epidemiology of the COVID-19 outbreak in Wuhan, China. *Jama*, 323(19):1915–1923, 2020.

[59] L. Tindale, M. Coombe, J.E. Stockdale, E. Garlock, W.Y.V. Lau, M. Saraswat, Y.B. Lee, L. Zhang, D. Chen, J. Wallinga, et al. Transmission interval estimates suggest pre-symptomatic spread of COVID-19. *MedRxiv*, 2020. DOI: 10.1101/2020.03.03.20029983.

[60] C. Jiehao, X. Jin, L. Daojiong, Y. Zhi, X. Lei, Q. Zhenghai, Z. Yuehua, Z. Hua, J. Ran, L. Pengcheng, et al. A case series of children with 2019 novel coronavirus infection: clinical and epidemiological features. *Clinical Infectious Diseases*, 71(6):1547–1551, 2020.

[61] R. Wöelfel, V.M. Corman, W. Guggemos, M. Seilmaier, S. Zange, M.A. Mueller, D. Niemeyer, P. Vollmar, C. Rothe, M. Hoelscher, et al. Virological assessment of hospitalized cases of coronavirus disease 2019. *MedRxiv*, 2020. DOI:10.1101/2020.03.05.20030502.

[62] R. Li, S. Pei, B. Chen, Y. Song, T. Zhang, W. Yang, and J. Shaman. Substantial undocumented infection facilitates the rapid dissemination of novel coronavirus (SARS-CoV-2). *Science*, 368(6490):489–493, 2020.

[63] Z. Wu and J.M. McGoogan. Characteristics of and important lessons from the coronavirus disease 2019 (COVID-19) outbreak in china: summary of a report of 72 314 cases from the chinese center for disease control and prevention. *Jama*, 323(13):1239–1242, 2020.

[64] W. Guan, Z. Ni, Y. Hu, W. Liang, C. Ou, J. He, L. Liu, H. Shan, C. Lei, et al. Clinical characteristics of coronavirus disease 2019 in china. *New England journal of medicine*, 382(18):1708–1720, 2020.

[65] S. Sanche, Y.T. Lin, C. Xu, E. Romero-Severson, N. Hengartner, and R. Ke. The Novel Coronavirus, 2019-nCoV, is Highly Contagious and More Infectious Than Initially Estimated. *medRxiv*, 2020. DOI: 10.1101/2020.02.07.20021154.

[66] L. Wang, Y. Gao, L. Lou, and G. Zhang. The clinical dynamics of 18 cases of COVID-19 outside of Wuhan, China. *European Respiratory Journal*, 55(4), 2000398. DOI: 10.1183/13993003.00398-2020.

[67] F. Pan, T. Ye, P. Sun, S. Gui, B. Liang, L. Li, D. Zheng, J. Wang, R.L. Hesketh, L. Yang, et al. Time course of lung changes on chest CT during recovery from 2019 novel coronavirus (COVID-19) pneumonia. *Radiology*, 295(3):715–721, 2020.

[68] W. Liu, Q. Zhang, J. Chen, R. Xiang, H. Song, S. Shu, L. Chen, L. Liang, J. Zhou, L. You, et al. Detection of covid-19 in children in early january 2020 in wuhan, china. *New England Journal of Medicine*, 382(14):1370–1371, 2020.

[69] R. Verity, L. Okell, I. Dorigatti, P. Winskill, C. Whittaker, et al. Estimates of the severity of coronavirus disease 2019: a model-based analysis. *The Lancet infectious diseases*, 20(6):669–677, 2020.

[70] N. Ferguson, D. Laydon, G. Nedjati-Gilani, N. Imai, K. Ainslie, M. Baguelin, S.Bhatia, A. Boonyasiri, Cucunubá Z, G.Cuomo-Dannenburg, et al. Report 9: Impact of non-pharmaceutical interventions (NPIs) to reduce COVID19 mortality and healthcare demand. *Imperial College London*, 10(77482):491–497, 2020.

[71] Staff Report. 100 days of Covid-19: The proactive steps UAE has taken so far. Retrieved May 3, 2020, from https://www.khaleejtimes.com/coronavirus-pandemic/100-days-of-covid-19-the-proactive-steps-uae-has-taken-so-far–.

[72] Mobility Trend Reports of Google. Retrieved June 29, 2020, from https://www.google.com/covid19/mobility/.

[73] Mobility Trend Reports of Apple. Retrieved June 29, 2020, from https://www.apple.com/covid19/mobility.

[74] Central Intelligence Agency. The World Fact Book: United Arab Emirates. Retrieved June 15, 2020, from https://www.cia.gov/the-world-factbook/countries/united-arab-emirates/.

Appendix

The mathematical formulas that have been used to calculate the initial parameter estimations of Model 6.1 are presented in Table 6.6.

Table 6.6: Formulas of the estimated parameter values

Parameter	Mathematical Formula
$\gamma_i, \ i = 1, 2$	$1/\text{PresPer}$
$\nu_i, \ i = 1, 2$	$1/(\text{IncPer-PresPer})$
$\kappa_i, \ i = 1, 2$	$(1/\text{DurA})\text{FracMInf}$
$\varphi_i, \ i = 1, 2$	0
$\alpha_{A_i}, \ i = 1, 2$	$(1/\text{DurA})(1 - \text{FracMInf})$
$\xi_i, \ i = 1, 2$	$(1/\text{DurMInf})\text{FracSev}$
$\alpha_{I_i}, \ i = 1, 2$	$(1/\text{DurMInf})(1 - \text{FracSev})$
η	$(1/\text{DurHos})\text{FracCri}$
α_J	$(1/\text{DurHos})(1 - \text{FracCri})$
α_C	$(1/\text{TimeICU})(1 - \text{ProbDeath})$
μ	$(1/\text{TimeICUdeath})\text{ProbDeath}$

The sensitivity of the *Basic Reproduction Number* $\mathscr{R}_0$ to the disease transmission parameters have the following formulas:

$$\Upsilon_{\beta_{A_1}^1}^{\mathscr{R}_0} = \frac{\partial \mathscr{R}_0}{\partial \beta_{A_1}^1} \frac{\beta_{A_1}^1}{\mathscr{R}_0} = \frac{1}{2} \left(\frac{2\mathscr{R}_{01}\phi_1 S_1^o - 2\mathscr{R}_{02}\phi_1 S_1^o}{2\sqrt{(\mathscr{R}_{01} - \mathscr{R}_{02})^2 + 4\bar{\mathscr{R}}_{01}\bar{\mathscr{R}}_{02}}} + \phi_1 S_1^o \right) \frac{\beta_{A_1}^1}{\mathscr{R}_0}$$

$$\Upsilon_{\beta_{A_2}^1}^{\mathscr{R}_0} = \frac{\partial \mathscr{R}_0}{\partial \beta_{A_2}^1} \frac{\beta_{A_2}^1}{\mathscr{R}_0} = \frac{1}{2} \left(\frac{4\bar{\mathscr{R}}_{02}\phi_3 S_1^o}{2\sqrt{(\mathscr{R}_{01} - \mathscr{R}_{02})^2 + 4\bar{\mathscr{R}}_{01}\bar{\mathscr{R}}_{02}}} \right) \frac{\beta_{A_2}^1}{\mathscr{R}_0}$$

$$\Upsilon_{\beta_{I_1}^1}^{\mathscr{R}_0} = \frac{\partial \mathscr{R}_0}{\partial \beta_{I_1}^1} \frac{\beta_{I_1}^1}{\mathscr{R}_0} = \frac{1}{2} \left(\frac{2\mathscr{R}_{01}\phi_2 S_1^o - 2\mathscr{R}_{02}\phi_2 S_1^o}{2\sqrt{(\mathscr{R}_{01} - \mathscr{R}_{02})^2 + 4\bar{\mathscr{R}}_{01}\bar{\mathscr{R}}_{02}}} + \phi_2 S_1^o \right) \frac{\beta_{I_1}^1}{\mathscr{R}_0}$$

$$\Upsilon_{\beta_{I_2}^1}^{\mathscr{R}_0} = \frac{\partial \mathscr{R}_0}{\partial \beta_{I_2}^1} \frac{\beta_{I_2}^1}{\mathscr{R}_0} = \frac{1}{2} \left(\frac{4\bar{\mathscr{R}}_{02}\phi_4 S_1^o}{2\sqrt{(\mathscr{R}_{01} - \mathscr{R}_{02})^2 + 4\bar{\mathscr{R}}_{01}\bar{\mathscr{R}}_{02}}} \right) \frac{\beta_{I_2}^1}{\mathscr{R}_0}$$

$$\Upsilon_{\beta_{A_1}^2}^{\mathscr{R}_0} = \frac{\partial \mathscr{R}_0}{\partial \beta_{A_1}^2} \frac{\beta_{A_1}^2}{\mathscr{R}_0} = \frac{1}{2} \left(\frac{4\bar{\mathscr{R}}_{01}\phi_1 S_2^o}{2\sqrt{(\mathscr{R}_{01} - \mathscr{R}_{02})^2 + 4\bar{\mathscr{R}}_{01}\bar{\mathscr{R}}_{02}}} \right) \frac{\beta_{A_1}^2}{\mathscr{R}_0}$$

$$\Upsilon_{\beta_{A_2}^2}^{\mathscr{R}_0} = \frac{\partial \mathscr{R}_0}{\partial \beta_{A_2}^2} \frac{\beta_{A_2}^2}{\mathscr{R}_0} = \frac{1}{2} \left(\frac{-2\mathscr{R}_{01}\phi_3 S_2^o + 2\mathscr{R}_{02}\phi_3 S_2^o}{2\sqrt{(\mathscr{R}_{01} - \mathscr{R}_{02})^2 + 4\bar{\mathscr{R}}_{01}\bar{\mathscr{R}}_{02}}} + \phi_3 S_2^o \right) \frac{\beta_{A_2}^2}{\mathscr{R}_0}$$

$$\Upsilon_{\beta_{I_1}^2}^{\mathscr{R}_0} = \frac{\partial \mathscr{R}_0}{\partial \beta_{I_1}^2} \frac{\beta_{I_1}^2}{\mathscr{R}_0} = \frac{1}{2} \left(\frac{4\bar{\mathscr{R}}_{01}\phi_1 S_2^o}{2\sqrt{(\mathscr{R}_{01} - \mathscr{R}_{02})^2 + 4\bar{\mathscr{R}}_{01}\bar{\mathscr{R}}_{02}}} \right) \frac{\beta_{I_1}^2}{\mathscr{R}_0}$$

$$\Upsilon_{\beta_{I_2}^2}^{\mathscr{R}_0} = \frac{\partial \mathscr{R}_0}{\partial \beta_{I_2}^2} \frac{\beta_{I_2}^2}{\mathscr{R}_0} = \frac{1}{2} \left(\frac{-2\mathscr{R}_{01}\phi_4 S_2^o + 2\mathscr{R}_{02}\phi_4 S_2^o}{2\sqrt{(\mathscr{R}_{01} - \mathscr{R}_{02})^2 + 4\bar{\mathscr{R}}_{01}\bar{\mathscr{R}}_{02}}} + \phi_4 S_2^o \right) \frac{\beta_{I_2}^2}{\mathscr{R}_0}$$

The sensitivity of the *Basic Reproduction Number* $\mathscr{R}_0$ to the disease transition parameters have the following formulas:

$$\Upsilon^{\mathscr{R}_0}_{\gamma_1} = \frac{\partial \mathscr{R}_0}{\partial \gamma_1}\frac{\gamma_1}{\mathscr{R}_0}$$

$$= \frac{1}{2}\left(\frac{\frac{2\mathscr{R}_{01}S^o_1 v_1}{(\gamma_1+v_1)^2}(\beta^1_{A_1}\phi_5+\beta^1_{I_1}\phi_6-\frac{\beta^1_{I_1}}{(\xi_1+\alpha_{I_1})})-\frac{2\mathscr{R}_{02}S^o_1 v_1}{(\gamma_1+v_1)^2}(\beta^1_{A_1}\phi_5+\beta^1_{I_1}\phi_6-\frac{\beta^1_{I_1}}{(\xi_1+\alpha_{I_1})})+\frac{4\bar{\mathscr{R}}_{01}S^o_2 v_1}{(\gamma_1+v_1)^2}(\beta^2_{A_1}\phi_5+\beta^2_{I_1}\phi_6-\frac{\beta^2_{I_1}}{(\xi_1+\alpha_{I_1})})}{2\sqrt{(\mathscr{R}_{01}-\mathscr{R}_{02})^2+4\bar{\mathscr{R}}_{01}\bar{\mathscr{R}}_{02}}}\right.$$
$$\left. + \frac{S^o_1 v_1}{(\gamma_1+v_1)^2}(\beta^1_{A_1}\phi_5+\beta^1_{I_1}\phi_6-\frac{\beta^1_{I_1}}{(\xi_1+\alpha_{I_1})})\right)\frac{\gamma_1}{\mathscr{R}_0}$$

$$\Upsilon^{\mathscr{R}_0}_{\gamma_2} = \frac{\partial \mathscr{R}_0}{\partial \gamma_2}\frac{\gamma_2}{\mathscr{R}_0}$$

$$= \frac{1}{2}\left(\frac{\frac{-2\mathscr{R}_{01}S^o_2 v_2}{(\gamma_2+v_2)^2}(\beta^2_{A_2}\phi_7+\beta^2_{I_2}\phi_8-\frac{\beta^2_{I_2}}{(\xi_2+\alpha_{I_2})})+\frac{4\bar{\mathscr{R}}_{02}S^o_1 v_2}{(\gamma_2+v_2)^2}(\beta^1_{A_2}\phi_7+\beta^1_{I_2}\phi_8-\frac{\beta^1_{I_2}}{(\xi_2+\alpha_{I_2})})+\frac{2\mathscr{R}_{02}S^o_2 v_2}{(\gamma_2+v_2)^2}(\beta^2_{A_2}\phi_7+\beta^2_{I_2}\phi_8-\frac{\beta^2_{I_2}}{(\xi_2+\alpha_{I_2})})}{2\sqrt{(\mathscr{R}_{01}-\mathscr{R}_{02})^2+4\bar{\mathscr{R}}_{01}\bar{\mathscr{R}}_{02}}}\right.$$
$$\left. + \frac{S^o_2 v_2}{(\gamma_2+v_2)^2}(\beta^2_{A_2}\phi_7+\beta^2_{I_2}\phi_8-\frac{\beta^2_{I_2}}{(\xi_2+\alpha_{I_2})})\right)\frac{\gamma_2}{\mathscr{R}_0}$$

$$\Upsilon^{\mathscr{R}_0}_{v_1} = \frac{\partial \mathscr{R}_0}{\partial v_1}\frac{v_1}{\mathscr{R}_0}$$

$$= \frac{1}{2}\left(\frac{\frac{2\mathscr{R}_{01}S^o_1 \gamma_1}{(\gamma_1+v_1)^2}(-\beta^1_{A_1}\phi_5-\beta^1_{I_1}\phi_6+\frac{\beta^1_{I_1}}{(\xi_1+\alpha_{I_1})})-\frac{2\mathscr{R}_{02}S^o_1 \gamma_1}{(\gamma_1+v_1)^2}(-\beta^1_{A_1}\phi_5-\beta^1_{I_1}\phi_6+\frac{\beta^1_{I_1}}{(\xi_1+\alpha_{I_1})})+\frac{4\bar{\mathscr{R}}_{01}S^o_2 \gamma_1}{(\gamma_1+v_1)^2}(-\beta^2_{A_1}\phi_5-\beta^2_{I_1}\phi_6+\frac{\beta^2_{I_1}}{(\xi_1+\alpha_{I_1})})}{2\sqrt{(\mathscr{R}_{01}-\mathscr{R}_{02})^2+4\bar{\mathscr{R}}_{01}\bar{\mathscr{R}}_{02}}}\right.$$
$$\left. + \frac{S^o_1 \gamma_1}{(\gamma_1+v_1)^2}(-\beta^1_{A_1}\phi_5-\beta^1_{I_1}\phi_6+\frac{\beta^1_{I_1}}{(\xi_1+\alpha_{I_1})})\right)\frac{v_1}{\mathscr{R}_0}$$

$$\Upsilon^{\mathscr{R}_0}_{v_2} = \frac{\partial \mathscr{R}_0}{\partial v_2}\frac{v_2}{\mathscr{R}_0}$$

$$= \frac{1}{2}\left(\frac{-\frac{2\mathscr{R}_{01}S^o_2 \gamma_2}{(\gamma_2+v_2)^2}(-\beta^2_{A_2}\phi_7-\beta^2_{I_2}\phi_8+\frac{\beta^2_{I_2}}{(\xi_2+\alpha_{I_2})})+\frac{4\bar{\mathscr{R}}_{02}S^o_1 \gamma_2}{(\gamma_2+v_2)^2}(-\beta^1_{A_2}\phi_7-\beta^1_{I_2}\phi_8+\frac{\beta^1_{I_2}}{(\xi_2+\alpha_{I_2})})+\frac{2\mathscr{R}_{02}S^o_2 \gamma_2}{(\gamma_2+v_2)^2}(-\beta^2_{A_2}\phi_7-\beta^2_{I_2}\phi_8+\frac{\beta^2_{I_2}}{(\xi_2+\alpha_{I_2})})}{2\sqrt{(\mathscr{R}_{01}-\mathscr{R}_{02})^2+4\bar{\mathscr{R}}_{01}\bar{\mathscr{R}}_{02}}}\right.$$
$$\left. + \frac{S^o_2 \gamma_2}{(\gamma_2+v_2)^2}(-\beta^2_{A_2}\phi_7-\beta^2_{I_2}\phi_8+\frac{\beta^2_{I_2}}{(\xi_2+\alpha_{I_2})})\right)\frac{v_2}{\mathscr{R}_0}$$

$$\Upsilon^{\mathscr{R}_0}_{\kappa_1} = \frac{\partial \mathscr{R}_0}{\partial \kappa_1}\frac{\kappa_1}{\mathscr{R}_0}$$

$$= \frac{1}{2}\left(\frac{\frac{\mathscr{R}_{01}S^o_1 \gamma_1 \phi^2_5}{(\gamma_1+v_1)}(-\beta^1_{A_1}+\frac{\beta^1_{I_1}(\varphi_1+\alpha_{A_1})}{(\xi_1+\alpha_{I_1})})-\frac{2\mathscr{R}_{02}S^o_1 \gamma_1 \phi^2_5}{(\gamma_1+v_1)}(-\beta^1_{A_1}+\frac{\beta^1_{I_1}(\varphi_1+\alpha_{A_1})}{(\xi_1+\alpha_{I_1})})+\frac{4\bar{\mathscr{R}}_{01}S^o_2 \gamma_1 \phi^2_5}{(\gamma_1+v_1)}(-\beta^2_{A_1}+\frac{\beta^2_{I_1}(\varphi_1+\alpha_{A_1})}{(\xi_1+\alpha_{I_1})})}{2\sqrt{(\mathscr{R}_{01}-\mathscr{R}_{02})^2+4\bar{\mathscr{R}}_{01}\bar{\mathscr{R}}_{02}}}\right.$$
$$\left. + \frac{S^o_1 \gamma_1 \phi^2_5}{(\gamma_1+v_1)}(-\beta^1_{A_1}+\frac{\beta^1_{I_1}(\varphi_1+\alpha_{A_1})}{(\xi_1+\alpha_{I_1})})\right)\frac{\kappa_1}{\mathscr{R}_0}$$

$$\Upsilon^{\mathscr{R}_0}_{\kappa_2} = \frac{\partial \mathscr{R}_0}{\partial \kappa_2}\frac{\kappa_2}{\mathscr{R}_0}$$

$$= \frac{1}{2}\left(\frac{-\frac{2\mathscr{R}_{01}S^o_2 \gamma_2 \phi^2_7}{(\gamma_2+v_2)}(-\beta^2_{A_2}+\frac{\beta^2_{I_2}(\varphi_2+\alpha_{A_2})}{(\xi_2+\alpha_{I_2})})+\frac{4\bar{\mathscr{R}}_{02}S^o_1 \gamma_2 \phi^2_7}{(\gamma_2+v_2)}(-\beta^1_{A_2}+\frac{\beta^1_{I_2}(\varphi_2+\alpha_{A_2})}{(\xi_2+\alpha_{I_2})})+\frac{2\mathscr{R}_{02}S^o_2 \gamma_2 \phi^2_7}{(\gamma_2+v_2)}(-\beta^2_{A_2}+\frac{\beta^2_{I_2}(\varphi_2+\alpha_{A_2})}{(\xi_2+\alpha_{I_2})})}{2\sqrt{(\mathscr{R}_{01}-\mathscr{R}_{02})^2+4\bar{\mathscr{R}}_{01}\bar{\mathscr{R}}_{02}}}\right.$$
$$\left. + \frac{S^o_2 \gamma_2 \phi^2_7}{(\gamma_2+v_2)}(-\beta^2_{A_2}+\frac{\beta^2_{I_2}(\varphi_2+\alpha_{A_2})}{(\xi_2+\alpha_{I_2})})\right)\frac{\kappa_2}{\mathscr{R}_0}$$

$$\Upsilon^{\mathscr{R}_0}_{\varphi_1} = \frac{\partial \mathscr{R}_0}{\partial \varphi_1}\frac{\varphi_1}{\mathscr{R}_0}$$

$$= \frac{1}{2}\left(\frac{\frac{2\mathscr{R}_{01}S^o_1 \gamma_1 \phi^2_5}{(\gamma_1+v_1)}(-\beta^1_{A_1}-\frac{\beta^1_{I_1}\kappa_1}{(\xi_1+\alpha_{I_1})})-\frac{2\mathscr{R}_{02}S^o_1 \gamma_1 \phi^2_5}{(\gamma_1+v_1)}(-\beta^1_{A_1}-\frac{\beta^1_{I_1}\kappa_1}{(\xi_1+\alpha_{I_1})})+\frac{4\bar{\mathscr{R}}_{01}S^o_2 \gamma_1 \phi^2_5}{(\gamma_1+v_1)}(-\beta^2_{A_1}-\frac{\beta^1_{I_1}\kappa_1}{(\xi_1+\alpha_{I_1})})}{2\sqrt{(\mathscr{R}_{01}-\mathscr{R}_{02})^2+4\bar{\mathscr{R}}_{01}\bar{\mathscr{R}}_{02}}}\right.$$
$$\left. + \frac{S^o_1 \gamma_1 \phi^2_5}{(\gamma_1+v_1)}(-\beta^1_{A_1}-\frac{\beta^1_{I_1}\kappa_1}{(\xi_1+\alpha_{I_1})})\right)\frac{\varphi_1}{\mathscr{R}_0}$$

$$\Upsilon_{\varphi_2}^{\mathscr{R}_0} = \frac{\partial \mathscr{R}_0}{\partial \varphi_2} \frac{\varphi_2}{\mathscr{R}_0}$$

$$= \frac{1}{2} \left(\frac{-\frac{2\mathscr{R}_{01} S_2^o \gamma_2 \phi_7^2}{(\gamma_2+v_2)} \left(-\beta_{A_2}^2 - \frac{\beta_{I_2}^2 \kappa_2}{(\xi_2+\alpha_{I_2})}\right) + \frac{4\mathscr{R}_{02} S_1^o \gamma_2 \phi_7^2}{(\gamma_2+v_2)} \left(-\beta_{A_2}^1 - \frac{\beta_{I_2}^1 \kappa_2}{(\xi_2+\alpha_{I_2})}\right) + \frac{2\mathscr{R}_{02} S_2^o \gamma_2 \phi_7^2}{(\gamma_2+v_2)} \left(-\beta_{A_2}^2 - \frac{\beta_{I_2}^2 \kappa_2}{(\xi_2+\alpha_{I_2})}\right)}{2\sqrt{(\mathscr{R}_{01}-\mathscr{R}_{02})^2 + 4\mathscr{R}_{01}\mathscr{R}_{02}}} \right.$$
$$\left. + \frac{S_2^o \gamma_2 \phi_7^2}{(\gamma_2+v_2)} \left(-\beta_{A_2}^2 - \frac{\beta_{I_2}^2 \kappa_2}{(\xi_2+\alpha_{I_2})}\right) \right) \frac{\varphi_2}{\mathscr{R}_0}$$

$$\Upsilon_{\alpha_{A_1}}^{\mathscr{R}_0} = \frac{\partial \mathscr{R}_0}{\partial \alpha_{A_1}} \frac{\alpha_{A_1}}{\mathscr{R}_0}$$

$$= \frac{1}{2} \left(\frac{\frac{2\mathscr{R}_{01} S_1^o \gamma_1 \phi_5^2}{(\gamma_1+v_1)} \left(-\beta_{A_1}^1 - \frac{\beta_{I_1}^1 \kappa_1}{(\xi_1+\alpha_{I_1})}\right) - \frac{2\mathscr{R}_{02} S_1^o \gamma_1 \phi_5^2}{(\gamma_1+v_1)} \left(-\beta_{A_1}^1 - \frac{\beta_{I_1}^1 \kappa_1}{(\xi_1+\alpha_{I_1})}\right) + \frac{4\mathscr{R}_{01} S_2^o \gamma_1 \phi_5^2}{(\gamma_1+v_1)} \left(-\beta_{A_1}^2 - \frac{\beta_{I_1}^1 \kappa_1}{(\xi_1+\alpha_{I_1})}\right)}{2\sqrt{(\mathscr{R}_{01}-\mathscr{R}_{02})^2 + 4\mathscr{R}_{01}\mathscr{R}_{02}}} \right.$$
$$\left. + \frac{S_1^o \gamma \phi_5^2}{(\gamma_1+v_1)} \left(-\beta_{A_1}^1 - \frac{\beta_{I_1}^1 \kappa_1}{(\xi_1+\alpha_{I_1})}\right) \right) \frac{\alpha_{A_1}}{\mathscr{R}_0}$$

$$\Upsilon_{\alpha_{A_2}}^{\mathscr{R}_0} = \frac{\partial \mathscr{R}_0}{\partial \alpha_{A_2}} \frac{\alpha_{A_2}}{\mathscr{R}_0}$$

$$= \frac{1}{2} \left(\frac{-\frac{2\mathscr{R}_{01} S_2^o \gamma_2 \phi_7^2}{(\gamma_2+v_2)} \left(-\beta_{A_2}^2 - \frac{\beta_{I_2}^2 \kappa_2}{(\xi_2+\alpha_{I_2})}\right) + \frac{4\mathscr{R}_{02} S_1^o \gamma_2 \phi_7^2}{(\gamma_2+v_2)} \left(-\beta_{A_2}^1 - \frac{\beta_{I_2}^1 \kappa_2}{(\xi_2+\alpha_{I_2})}\right) + \frac{2\mathscr{R}_{02} S_2^o \gamma_2 \phi_7^2}{(\gamma_2+v_2)} \left(-\beta_{A_2}^2 - \frac{\beta_{I_2}^2 \kappa_2}{(\xi_2+\alpha_{I_2})}\right)}{2\sqrt{(\mathscr{R}_{01}-\mathscr{R}_{02})^2 + 4\mathscr{R}_{01}\mathscr{R}_{02}}} \right.$$
$$\left. + \frac{S_2^o \gamma_2 \phi_7^2}{(\gamma_2+v_2)} \left(-\beta_{A_2}^2 - \frac{\beta_{I_2}^2 \kappa_2}{(\xi_2+\alpha_{I_2})}\right) \right) \frac{\alpha_{A_2}}{\mathscr{R}_0}$$

$$\Upsilon_{\xi_1}^{\mathscr{R}_0} = \frac{\partial \mathscr{R}_0}{\partial \xi_1} \frac{\xi_1}{\mathscr{R}_0}$$

$$= \frac{1}{2} \left(\frac{\frac{2\mathscr{R}_{01} S_1^o \beta_{I_1}^1}{(\gamma_1+v_1)(\xi_1+\alpha_{I_1})} \left(-\phi_6 \gamma_1 - \frac{v_1}{(\xi_1+\alpha_{I_1})}\right) - \frac{2\mathscr{R}_{02} S_1^o \beta_{I_1}^1}{(\gamma_1+v_1)(\xi_1+\alpha_{I_1})} \left(-\phi_6 \gamma_1 - \frac{v_1}{(\xi_1+\alpha_{I_1})}\right) + \frac{4\mathscr{R}_{01} S_2^o \beta_{I_1}^2}{(\gamma_1+v_1)(\xi_1+\alpha_{I_1})} \left(-\phi_6 \gamma_1 - \frac{v_1}{(\xi_1+\alpha_{I_1})}\right)}{2\sqrt{(\mathscr{R}_{01}-\mathscr{R}_{02})^2 + 4\mathscr{R}_{01}\mathscr{R}_{02}}} \right.$$
$$\left. + \frac{S_1^o \beta_{I_1}^1}{(\gamma_1+v_1)(\xi_1+\alpha_{I_1})} \left(-\phi_6 \gamma_1 - \frac{v_1}{(\xi_1+\alpha_{I_1})}\right) \right) \frac{\xi_1}{\mathscr{R}_0}$$

$$\Upsilon_{\xi_2}^{\mathscr{R}_0} = \frac{\partial \mathscr{R}_0}{\partial \xi_2} \frac{\xi_2}{R_0}$$

$$= \frac{1}{2} \left(\frac{-\frac{2\mathscr{R}_{01} S_2^o \beta_{I_2}^2}{(\gamma_2+v_2)(\xi_2+\alpha_{I_2})} \left(-\gamma_2 \phi_8 - \frac{v_2}{(\xi_2+\alpha_{I_2})}\right) + \frac{4\mathscr{R}_{02} S_1^o \beta_{I_2}^1}{(\gamma_2+v_2)(\xi_2+\alpha_{I_2})} \left(-\gamma_2 \phi_8 - \frac{v_2}{(\xi_2+\alpha_{I_2})}\right) + \frac{2\mathscr{R}_{02} S_2^o \beta_{I_2}^2}{(\gamma_2+v_2)(\xi_2+\alpha_{I_2})} \left(-\gamma_2 \phi_8 - \frac{v_2}{(\xi_2+\alpha_{I_2})}\right)}{2\sqrt{(\mathscr{R}_{01}-\mathscr{R}_{02})^2 + 4\mathscr{R}_{01}\mathscr{R}_{02}}} \right.$$
$$\left. + \frac{S_2^o \beta_{I_2}^2}{(\gamma_2+v_2)(\xi_2+\alpha_{I_2})} \left(-\gamma_2 \phi_8 - \frac{v_2}{(\xi_2+\alpha_{I_2})}\right) \right) \frac{\xi_2}{R_0}$$

$$\Upsilon_{\alpha_{I_1}}^{\mathscr{R}_0} = \frac{\partial \mathscr{R}_0}{\partial \alpha_{I_1}} \frac{\alpha_{I_1}}{\mathscr{R}_0}$$

$$= \frac{1}{2} \left(\frac{\frac{2\mathscr{R}_{01} S_1^o \beta_{I_1}^1}{(\gamma_1+v_1)(\xi_1+\alpha_{I_1})} \left(-\phi_6 \gamma_1 - \frac{v_1}{(\xi_1+\alpha_{I_1})}\right) - \frac{2\mathscr{R}_{02} S_1^o \beta_{I_1}^1}{(\gamma_1+v_1)(\xi_1+\alpha_{I_1})} \left(-\phi_6 \gamma_1 - \frac{v_1}{(\xi_1+\alpha_{I_1})}\right) + \frac{4\mathscr{R}_{01} S_2^o \beta_{I_1}^2}{(\gamma_1+v_1)(\xi_1+\alpha_{I_1})} \left(-\phi_6 \gamma_1 - \frac{v_1}{(\xi_1+\alpha_{I_1})}\right)}{2\sqrt{(\mathscr{R}_{01}-\mathscr{R}_{02})^2 + 4\mathscr{R}_{01}\mathscr{R}_{02}}} \right.$$
$$\left. + \frac{S_1^o \beta_{I_1}^1}{(\gamma_1+v_1)(\xi_1+\alpha_{I_1})} \left(-\phi_6 \gamma_1 - \frac{v_1}{(\xi_1+\alpha_{I_1})}\right) \right) \frac{\alpha_{I_1}}{\mathscr{R}_0}$$

$$\Upsilon_{\alpha_{I_2}}^{\mathscr{R}_0} = \frac{\partial \mathscr{R}_0}{\partial \alpha_{I_2}} \frac{\alpha_{I_2}}{\mathscr{R}_0}$$

$$= \frac{1}{2} \left(\frac{-\frac{2\mathscr{R}_{01} S_2^o \beta_{I_2}^2}{(\gamma_2+v_2)(\xi_2+\alpha_{I_2})} \left(-\gamma_2 \phi_8 - \frac{v_2}{(\xi_2+\alpha_{I_2})}\right) + \frac{4\mathscr{R}_{02} S_1^o \beta_{I_2}^1}{(\gamma_2+v_2)(\xi_2+\alpha_{I_2})} \left(-\gamma_2 \phi_8 - \frac{v_2}{(\xi_2+\alpha_{I_2})}\right) + \frac{2\mathscr{R}_{02} S_2^o \beta_{I_2}^2}{(\gamma_2+v_2)(\xi_2+\alpha_{I_2})} \left(-\gamma_2 \phi_8 - \frac{v_2}{(\xi_2+\alpha_{I_2})}\right)}{2\sqrt{(\mathscr{R}_{01}-\mathscr{R}_{02})^2 + 4\mathscr{R}_{01}\mathscr{R}_{02}}} \right.$$
$$\left. + \frac{S_2^o \beta_{I_2}^2}{(\gamma_2+v_2)(\xi_2+\alpha_{I_2})} \left(-\gamma_2 \phi_8 - \frac{v_2}{(\xi_2+\alpha_{I_2})}\right) \right) \frac{\alpha_{I_2}}{\mathscr{R}_0}$$

Note: The sensitivity indices of the remaining parameters are zero since $\mathscr{R}_0$ doesn't depend on them.